axioms

MDPI

Article

A Mathematical Model for Zika Virus Infection and Microcephaly Risk Considering Sexual and Vertical Transmission

Mahmoud A. Ibrahim [1,2,*] and Attila Dénes [1]

[1] National Laboratory for Health Security, Bolyai Institute, University of Szeged, Aradi vértanúk tere 1, 6720 Szeged, Hungary
[2] Department of Mathematics, Faculty of Science, Mansoura University, Mansoura 35516, Egypt
* Correspondence: mibrahim@math.u-szeged.hu

Abstract: We establish a compartmental model for Zika virus disease transmission, with particular attention paid to microcephaly, the main threat of the disease. To this end, we consider separate microcephaly-related compartments for affected infants, as well as the role of asymptomatic carriers, the influence of seasonality and transmission through sexual contact. We determine the basic reproduction number of the corresponding time-dependent model and time-constant model and study the dependence of this value on the mosquito-related parameters. In addition, we demonstrate the global stability of the disease-free periodic solution if $\mathcal{R}_0 < 1$, whereas the disease persists when $\mathcal{R}_0 > 1$. We fit our model to data from Colombia between 2015 and 2017 as a case study. The fitting is used to figure out how sexual transmission affects the number of cases among women as well as the number of microcephaly cases. Our sensitivity analyses conclude that the most effective ways to prevent Zika-related microcephaly cases are preventing mosquito bites and controlling mosquito populations, as well as providing protection during sexual contact.

Keywords: non-autonomous epidemic model; Zika fever; microcephaly; basic reproduction number

MSC: 34C23; 34C25; 34C60; 37N25; 92D25; 92D30

Citation: Ibrahim, M.A.; Dénes, A. A Mathematical Model for Zika Virus Infection and Microcephaly Risk Considering Sexual and Vertical Transmission. *Axioms* **2023**, *12*, 263. https://doi.org/10.3390/axioms12030263

Academic Editor: Behzad Djafari-Rouhani

Received: 14 January 2023
Revised: 15 February 2023
Accepted: 23 February 2023
Published: 3 March 2023

1. Introduction

Zika fever or Zika virus disease (ZIKV) is an arthropod-borne disease caused by a *Flavivirus*, mainly spread by infected female mosquito bites. The species responsible for transmission are primarily *Aedes aegypti* and *Aedes albopictus* [1]. Unlike other arboviruses, Zika can also be transmitted via sexual contact, primarily from males to females [2]. Evidence shows that ZIKV remains in semen up to six months, which is longer than it can remain in other bodily fluids. This means that the disease can still be transmitted several months after recovery [3]. The most common way for Zika to be transmitted is from a pregnant woman to her child. This has been shown to cause microcephaly and other serious fetal brain deficiencies although, historically, Zika fever was thought to have mild symptoms in humans, such as moderate fever, conjunctivitis, rash and joint discomfort. The Zika virus was first isolated in 1947 in a rhesus monkey in the Zika forest (Uganda). It was shown that the virus is transmitted between primates and mosquitoes, especially the mosquito species *Aedes africanus* [4]. At the end of 2015, the European Centre for Disease Prevention and Control published a study on the possible connection between Zika fever, congenital microcephaly and Guillain–Barré syndrome [5,6]. For example, in Brazil, 2782 microcephaly cases were reported in the year following the emergence of Zika fever, while there were only 147 and 167 cases in the two preceding years [7]. ZIKV was found to have been transmitted intrauterine for the first time in Brazil, in the uteri of two pregnant women whose fetuses were born with microcephaly. In Colombia, a total of 19,993 female

pregnant women with presumed Zika virus disease were recorded from the start of the epidemic up to week 33 of 2017, of whom 6365 were laboratory-confirmed with Zika virus infection [8,9]. In total, 1415 occurrences of microcephaly and other congenital disorders of the central nervous system were recorded in Colombia between the first week of 2016 and week 33 of 2017. Among these, 196 were laboratory-confirmed as being associated with Zika virus infection. The number of cases having microcephaly reveals an increasing trend in 2016, reaching its high in week 28. Whereas the number of cases has been decreasing since, in comparison to the same period 2014 and 2015, the trend has nevertheless shown a greater number of cases. In [10], the authors confirmed the link between microcephaly and congenital Zika infection based on a case–control investigation in 2016. The study [11], using data from national reporting databases in Brazil, also confirmed that congenital Zika infection, in particular in the first six months of pregnancy, can be linked with microcephaly and with other birth defects. Ref. [12] found that the number of Guillain–Barré syndrome patients increased parallelly with the number of Zika cases, while microcephaly cases appeared five months after the beginning of the outbreak, showing a functional relationship between the transmission of Zika fever and the increase of microcephaly and Guillain–Barré syndrome cases. Microcephaly was linked to other problems, such as miscarriage, stillbirth and other birth defects [13].

Several researchers have studied the dynamics of the Zika virus spread using mathematical models. Ref. [14] established a compartmental model that includes mosquito-borne spread and sexual transmission as well. In this paper, males and females were not differentiated. Ref. [15] formulated and analysed five compartmental models of Zika transmission, modelling heterogeneity in sexual transmission in several different ways. Saad-Roy, Ma and van den Driessche [16] introduced a model differentiating humans w.r.t. their sex and sexual activity. Some studies also consider the changes in the weather and climate in the models, see, e.g., [17–21]. A model for the transmission of the ZIKV presented in [22] also includes the effect of the periodicity of weather. This model included time-dependent mosquito parameters. The global dynamics are determined by the basic reproduction number $\mathcal{R}_0$: the disease-free equilibrium is shown to be globally asymptotically stable if $\mathcal{R}_0 < 1$, whereas when $\mathcal{R}_0 > 1$ the disease persists in the population. The model studied in [23] incorporated vertical transmission of the Zika virus among humans, the birth of newborns having microcephaly and asymptomatic carriers of the virus. In [24], a non-autonomous model was developed that took into account the majority of the important aspects of Zika spread: vector-borne and sexual transmission, the prolonged time of infectiousness following recovery, the role of asymptomatically infected persons, and the significance of weather seasonality. As the main concern regarding Zika infections is the possibility of malformations in newborns, a particular emphasis was put on the assessment of the effect of the epidemic on women.

In the current study, we extend the compartmental model described in [24] by taking into account the vertical transmission of Zika to the fetus in the early stages of pregnancy in order to better estimate the risk of microcephaly due to Zika. We determine the basic reproduction number of the corresponding time-dependent model using different methods. In addition, we demonstrate the global stability of the disease-free periodic solution in the case $\mathcal{R}_0 < 1$, whereas the disease persists when $\mathcal{R}_0 > 1$. To support the theoretical conclusions, numerical simulations are provided. In addition, we fit our model to data from Colombia between 2015 and 2017 as a case study.

2. Methods

2.1. Seasonal Compartmental Model

To account for sexual, vector-borne and vertical transmission, we divided the whole human population N_h into three categories: adult females, denoted by N_f, adult males, denoted by N_m, and children, denoted by N_c and consisting of newly born babies and children under puberty. In order to simplify our model, we do not introduce separate compartments for pregnant women, but we assume that a constant percentage of women (in any of the

adult female compartments) is pregnant at any time t. Susceptible humans (S_f, S_m and S_c) are those who can be infected by the Zika virus. Once having contracted the disease, individuals progress to the exposed compartment (E_f, E_m and E_c), and these persons do not have any symptoms yet. If a person has been exposed to the Zika virus but has not yet developed symptoms or been confirmed as infected, they can still potentially spread the virus to others. This is because the virus can be present in the blood (viraemia) and semen (virusemenia) of an infected person for a period of time before symptoms appear [14,25]. Following the incubation time, exposed humans transfer to one of the symptomatically infected classes (I_f^s, I_m^s, I_c^s) and the asymptomatically infected compartments (I_f^a, I_m^a, I_c^a), based on whether that person shows symptoms or not. Both asymptomatically and symptomatically infected adult males progress to the convalescent class (I_m^r) which includes individuals who have recovered from the disease but are still able to spread it through sexual contact. For adult females, we introduce the compartment I_f^r. A percentage of those in I_f^r are those recovered mothers who had Zika during their pregnancy. Children of women who were previously infected by Zika might develop microcephaly and be born into the M_c class, or they might be born healthy and thus arrive at the recovered compartment R_c. To incorporate the time from infection of the mother to birth, we introduce a time delay (τ), which in our model is given as a constant delay based on the average time between infection and delivery of mothers who have given birth to babies with microcephaly. Adults enter the recovered classes (R_f, R_m) after the convalescent phase. Infected mothers' children who are born healthy will move to the recovered compartment R_c, while those who develop microcephaly will move to compartment M_c. The Zika virus only causes microcephaly during pregnancy and not after birth in non-infected children. It only affects the developing fetal brain leading to abnormal brain development and microcephaly in some newborns. Children who were not infected during pregnancy are not at risk of developing microcephaly [26]. Once the infected children have recovered, they will be transferred to the recovered compartment. We point out that the infectious classes (E, I^s, I^a, I^r) also differ in terms of recovery and transmission rates. We introduce three mosquito compartments: susceptible (S_v), exposed (E_v) and infected (I_v). Figure 1 depicts the model's transmission diagram.

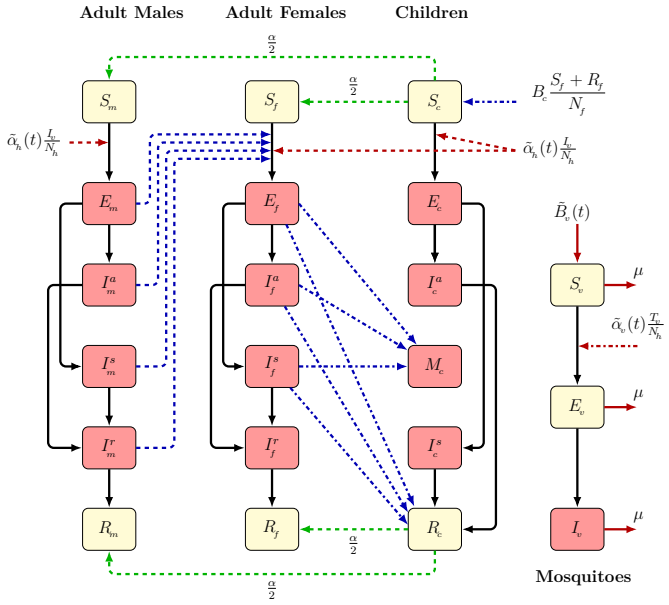

Figure 1. The dynamics of the spread of the Zika virus, taking into account three human groups, and sexual, vertical and vectorial transmission. Adult males, adult females, children and mosquitoes are denoted by the lower indices m, f, c and v, respectively. Yellow nodes denote non-infectious and red nodes denote infectious compartments. The disease progression is depicted by black, solid arrows. The direction of sexual transmission from adult males to adult females is shown by blue dashed arrows, while blue dash–dotted arrows illustrate the direction of vertical infection from adult females to their children. Green dashed arrows show the direction of the maturation from child to adult. Red dashed lines show the direction of mosquito-to-human transmission.

The total human population is $N_h(t) = N_f(t) + N_m(t) + N_c(t)$ and the total population for each group is given as:

$$\begin{aligned} N_f(t) &= S_f(t) + E_f(t) + I_f^a(t) + I_f^s(t) + I_f^r(t) + R_f(t), \\ N_m(t) &= S_m(t) + E_m(t) + I_m^a(t) + I_m^s(t) + I_m^r(t) + R_m(t), \\ N_c(t) &= S_c(t) + E_c(t) + I_c^a(t) + I_c^s(t) + M_c(t) + R_c(t), \end{aligned}$$

while the total mosquito population is given by $N_v(t) = S_v(t) + E_v(t) + I_v(t)$.

In accordance with the transmission diagram in Figure 1 and the parameter description given in Table 1, the mathematical model takes the form

$$
\begin{aligned}
&\text{Adult females}\begin{cases}
S_f'(t) = \frac{\alpha}{2}S_c(t) - \beta\frac{T_h(t)}{N_f(t)}S_f(t) - \tilde{\alpha}_h(t)\frac{I_v(t)}{N_h(t)}S_f(t) - dS_f(t),\\
E_f'(t) = \beta\frac{T_h(t)}{N_f(t)}S_f(t) + \tilde{\alpha}_h(t)\frac{I_v(t)}{N_h(t)}S_f(t) - (\nu_h + d)E_f(t),\\
I_f^{a\prime}(t) = \theta\nu_h E_f(t) - \gamma_a I_f^a(t) - dI_f^a(t),\\
I_f^{s\prime}(t) = (1-\theta)\nu_h E_f(t) - \gamma_s I_f^s(t) - dI_f^s(t),\\
I_f^{r\prime}(t) = \gamma_a I_f^a(t) + \gamma_s I_f^s(t) - \gamma_r I_f^r(t) - dI_f^r(t),\\
R_f'(t) = \frac{\alpha}{2}R_c(t) + \gamma_r I_f^r(t) - dR_f(t),
\end{cases}\\
&\text{Adult males}\begin{cases}
S_m'(t) = \frac{\alpha}{2}S_c(t) - \tilde{\alpha}_h(t)\frac{I_v(t)}{N_h(t)}S_m(t) - dS_m(t),\\
E_m'(t) = \tilde{\alpha}_h(t)\frac{I_v(t)}{N_h(t)}S_m(t) - (\nu_h + d)E_m(t),\\
I_m^{a\prime}(t) = \theta\nu_h E_m(t) - \gamma_a I_m^a(t) - dI_m^a(t),\\
I_m^{s\prime}(t) = (1-\theta)\nu_h E_m(t) - \gamma_s I_m^s(t) - dI_m^s(t),\\
I_m^{r\prime}(t) = \gamma_a I_m^a(t) + \gamma_s I_m^s(t) - \gamma_r I_m^r(t) - dI_m^r(t),\\
R_m'(t) = \frac{\alpha}{2}R_c(t) + \gamma_r I_m^r(t) - dR_m(t),
\end{cases}\\
&\text{Children}\begin{cases}
S_c'(t) = B_c\frac{S_f(t-\tau)+R_f(t-\tau)}{N_f(t-\tau)}e^{-\xi\tau} - \tilde{\alpha}_h(t)\frac{I_v(t)}{N_h(t)}S_c(t) - \alpha S_c(t) - \xi S_c(t),\\
E_c'(t) = \tilde{\alpha}_h(t)\frac{I_v(t)}{N_h(t)}S_c(t) - \nu_h E_c(t) - \xi E_c(t),\\
I_c^{a\prime}(t) = \theta\nu_h E_c(t) - \gamma_a I_c^a(t) - \xi I_c^a(t),\\
I_c^{s\prime}(t) = (1-\theta)\nu_h E_c(t) - \gamma_s I_c^s(t) - \xi I_c^s(t),\\
M_c'(t) = (1-p)B_c\frac{E_f(t-\tau)+I_f^a(t-\tau)+I_f^s(t-\tau)}{N_f(t-\tau)}e^{-\xi\tau} - \xi M_c(t),\\
R_c'(t) = pB_c\frac{E_f(t-\tau)+I_f^a(t-\tau)+I_f^s(t-\tau)}{N_f(t-\tau)}e^{-\xi\tau} + \gamma_a I_c^a(t) + \gamma_s I_c^s(t) - \alpha R_c(t) - \xi R_c(t),
\end{cases}\\
&\text{Mosquitoes}\begin{cases}
S_v'(t) = \tilde{B}_v(t) - \tilde{\alpha}_v(t)\frac{T_v(t)}{N_h(t)}S_v(t) - \mu S_v(t),\\
E_v'(t) = \tilde{\alpha}_v(t)\frac{T_v(t)}{N_h(t)}S_v(t) - (\nu_v + \mu)E_v(t),\\
I_v'(t) = \nu_v E_v(t) - \mu I_v(t),
\end{cases}
\end{aligned}
\tag{1}
$$

where

$$
\begin{aligned}
T_h(t) &= \kappa_e E_m(t) + \kappa_a I_m^a(t) + I_m^s(t) + \kappa_r I_m^r(t),\\
T_v(t) &= \eta_e\big(E_f(t) + E_m(t) + E_c(t)\big) + \eta_a\big(I_f^a(t) + I_m^a(t) + I_c^a(t)\big) + I_f^s(t) + I_m^s(t) + I_c^s(t),
\end{aligned}
$$

and all other parameter descriptions are summarized in Table 1. In particular, B_c and ξ are children's birth and death rates, d is the adult death rate and β is the rate at which symptomatic males spread the disease to susceptible females; β multiplied by κ_e, κ_a and κ_r yields the rates at which exposed, asymptotically infected and convalescent men spread the disease to women, respectively. The fraction of asymptomatically infected individuals is represented by θ.

Table 1. Description of the model (1) parameters.

Parameter	Description
B_c	Natural birth rate of children
ξ	Natural death rate of children
α	Maturation rate
d	Natural death rate of adults
β	Transmission rate from human to human
α_h	Baseline value of mosquito-to-human transfer rate
α_v	Baseline value of humans-to-mosquito transfer rate
θ	Ratio of asymptomatic infections
$\kappa_e, \kappa_a, \kappa_r$	Relative transmissibility of exposed humans to infectious humans
η_e, η_a	Relative transmissibility of infectious human to mosquitoes
γ_a	Progression rate from I^a to I^r
γ_s	Progression rate from I^s to I^r
γ_r	Recovery rate of convalescent humans
ν_h	Human incubation rate
ν_v	Incubation rate in mosquitoes
B_v	Baseline value of mosquito birth rate
μ	Mosquito death rate
p	Fraction of children who have recovered
$1-p$	Fraction of children who have microcephaly
a, b	Seasonality parameters
τ	Constant delay

Humans have a latent period of $1/\nu$ length and the infection periods are as follows: $1/\gamma_a, 1/\gamma_s$ and $1/\gamma_s$. The period $1/\gamma_r$ represents the length of time that recovered men are still infectious through sexual contact and recovered women are still infectious during pregnancy. The functions $\tilde{\alpha}_h(t)$, $\tilde{\alpha}_v(t)$ and $\tilde{B}_v(t)$ represent, respectively, the transmission rate from an infected mosquito to a susceptible person, the transmission rate from an infected human to a susceptible mosquito and the birth rate of mosquitoes. These functions are considered to be time-periodic, with one year serving as the period and following for instance [22,24,27] they are expected to be of the form $\alpha_h \cdot \left(\sin\left(\frac{2\pi}{P}t + b\right) + a\right)$, $\alpha_v \cdot \left(\sin\left(\frac{2\pi}{P}t + b\right) + a\right)$ and $B_v \cdot \left(\sin\left(\frac{2\pi}{P}t + b\right) + a\right)$ where P represents the length of the period, a and b are free adjustment parameters, and α_h, α_v, B_v denote the (constant) baseline values of the time-dependent parameters, respectively. Just like in the case of human-to-human transmission, we also introduce the modification parameters η_e, η_a for the infectiousness of exposed and asymptomatically infected people, respectively. We have $1/\nu_v$ for the length of the latent period for mosquitoes, while the average life span of mosquitoes is given by $1/\mu$.

2.2. Zika Fever and Microcephaly Cases Data

The public and freely available weekly ZIKV confirmed cases were collected from the National Health Institute of Colombia [28–30] and Pan American Health Organization [31,32]. We focus our analysis on 2015–2017 confirmed ZIKV cases since the start of the epidemic on week 33 of 2015 up to week 33 of 2017, while for microcephaly we use the data starting from week 33 of 2015 up to week 3 of 2017. There was a delay between the mother's infection and the delivery which caused the lag time between the peaks observed in the number of symptomatically infected cases and microcephaly cases. Figure 2a shows the weekly confirmed cases of the 2015–2017 ZIKV outbreak in Colombia. Figure 2b shows the weekly confirmed microcephaly cases of 2015–2017 in Colombia.

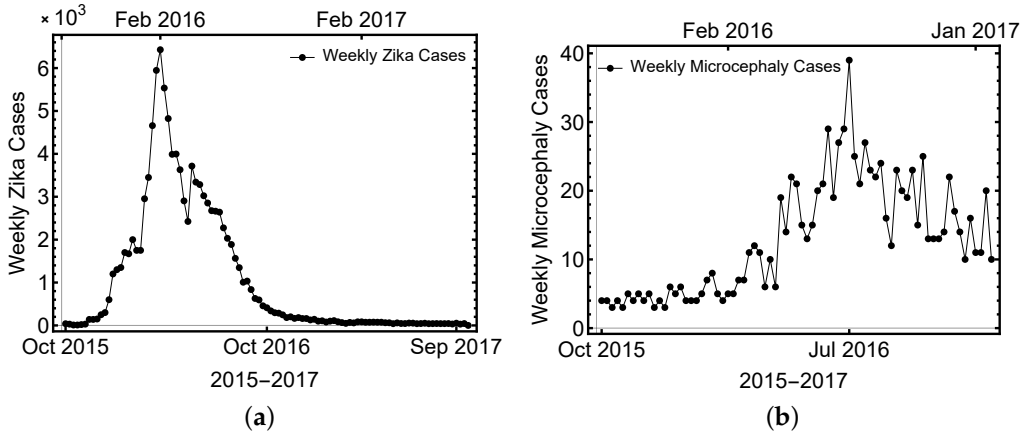

Figure 2. Colombia, weekly distribution of ZIKV and microcephaly cases, 2015–2017. (**a**) Weekly Zika cases. (**b**) Weekly microcephaly cases.

2.3. Parameter Estimation, Sensitivity and Reproduction Numbers

To calculate the parameters of model (1) providing the most satisfactory fit to data, we use Latin hypercube sampling. This sampling method is used to simultaneously measure the variance in various parameter values (see, e.g., [33] for details). The main idea of the method is to generate a representative sample set from the ranges for all fitted parameters. To obtain a representative sample set of size m, the parameter ranges are divided into m equal subintervals and one point is selected from each subinterval. After obtaining the m lists of samples, they are combined randomly into m-tuples. For each element of this sample set, the solutions of the model (1) are numerically calculated. Finally, we apply the least squares method to find the parameters providing the best fit. In order to classify the parameters w.r.t. their influence on the number of microcephaly cases, we employ partial rank correlation coefficients estimation (PRCC, see, e.g., [34]), to perform sensitivity analysis. When we change the parameters within the predetermined ranges, the PRCC-based sensitivity analysis assesses the impact of the parameters on the response function (in our case, the number of microcephaly cases). Higher positive (or negative) PRCC values indicate that a parameter has a positive (or negative) correlation with the outcome function.

The basic reproduction number ($\mathcal{R}_0$) of a periodic mathematical model can be determined as the spectral radius of a linear integral operator on a set of time-dependent functions (see [35], for details). Although the value of $\mathcal{R}_0$ cannot be computed analytically, there are methods to do it numerically (see, e.g., [36] for details). There are also interesting results from calculating the basic reproduction number as a time average for the corresponding periodic model. Setting the time-dependent parameters (mosquito birth rate and bite rates) to constant yields the formula for the time-average basic reproduction number, which can be found in (12). In addition to the basic reproduction number ($\mathcal{R}_0$), the instantaneous reproduction rate, $\mathcal{R}_{inst}$, which measures the average number of secondary cases per infectious case in a population, can be computed by multiplying $\mathcal{R}_0$ by the size of the susceptible percentage of the host population.

3. Results

3.1. Threshold Dynamics

We present some notations for studying the existence of solutions to the system (1) as well as the uniqueness of those solutions. For a certain continuous ω-periodic function $h(t)$, we introduce $\hat{h} = \sup_{t\in[0,\omega)} h(t)$.

Let

$$C := C\big([-\tau, 0], \mathbb{R}^6\big) \times \mathbb{R}^{15},$$
$$C^+ := C\big([-\tau, 0], \mathbb{R}^6_+\big) \times \mathbb{R}^{15}_+.$$

Thus (C, C^+) defines an ordered Banach space together with the maximum norm. If $x = (x_1, x_2, \ldots, X_{21}) : [-\tau, \sigma] \to \mathbb{R}^{21}_+$ is continuous function with $\sigma > 0$, then, for any $t \in [0, \sigma)$, we define $x_t \in C$ to be $x_t(\theta) = \big(x_1(t+\theta), x_2(t+\theta), x_3(t+\theta), x_4(t+\theta), x_5(t+\theta), x_6(t+\theta), x_7(t), x_8(t), \ldots, x_{21}(t)\big), \forall\, \theta \in [-\tau, 0]$.

Define

$$\Omega := \left\{ \phi \in C^+ : \begin{array}{l} \phi_i(\theta) \geqslant 0,\ i = \{1, 2, \ldots, 6\},\ \ \forall\, \theta \in [-\tau, 0], \\ \phi_j \geqslant 0,\ j = \{7, 8, \ldots, 21\}. \end{array} \right\}.$$

Lemma 1. *Equation* (1) *has a unique non-negative bounded solution* $u(t, \phi)$ *on* $[0, \infty)$ *with* $u_0 = \phi$, *for any* $\phi \in \Omega$, *such that* $u_t(\phi) \in \Omega$ *for all* $t \geqslant 0$.

Proof. We introduce the following matrix function $\tilde{f}(t, \phi)$, for any $\phi = (\phi_1, \phi_2, \ldots, \phi_{21}) \in \Omega$, as follows:

$$\tilde{f}(t,\phi) = \begin{pmatrix} \frac{\alpha}{2}\phi_{13}(0) - \beta\frac{T_h(0)}{N_f}\phi_1(0) - \frac{\tilde{\alpha}_h(t)\phi_{21}(0)}{N_h}\phi_1(0) - d\phi_1(0) \\ \beta\frac{T_h(0)}{N_f}\phi_1(0) + \frac{\tilde{\alpha}_h(t)\phi_{21}(0)}{N_h}\phi_1(0) - (\nu_h + d)\phi_2(0) \\ \theta\nu_h\phi_2(0) - \gamma_a\phi_3(0) - d\phi_3(0) \\ (1-\theta)\nu_h\phi_2(0) - \gamma_s\phi_4(0) - d\phi_4(0) \\ \gamma_a\phi_3(0) + \gamma_s\phi_4(0) - \gamma_r\phi_5(0) - d\phi_5(0) \\ \frac{\alpha}{2}\phi_{18}(0) + \gamma_r\phi_5(0) - d\phi_6(0) \\ \frac{\alpha}{2}\phi_{13}(0) - \frac{\tilde{\alpha}_h(t)\phi_{21}(0)}{N_h}\phi_7(0) - d\phi_7(0) \\ \frac{\tilde{\alpha}_h(t)\phi_{21}(0)}{N_h}\phi_7(0) - (\nu_h + d)\phi_8(0) \\ \theta\nu_h\phi_8(0) - \gamma_a\phi_9(0) - d\phi_9(0) \\ (1-\theta)\nu_h\phi_8(0) - \gamma_s\phi_{10}(0) - d\phi_{10}(0) \\ \gamma_a\phi_9(0) + \gamma_s\phi_{10}(0) - \gamma_r\phi_{11}(0) - d\phi_{11}(0) \\ \frac{\alpha}{2}\phi_{18}(0) + \gamma_r\phi_{11}(0) - d\phi_{12}(0) \\ B_c\frac{\phi_1(-\tau)+\phi_6(-\tau)}{N_f}e^{-\xi\tau} - \frac{\tilde{\alpha}_h(t)\phi_{21}(0)}{N_h}\phi_{13}(0) - \alpha\phi_{13}(0) - \xi\phi_{13}(0) \\ \frac{\tilde{\alpha}_h(t)\phi_{21}(0)}{N_h}\phi_{13}(0) - \nu_h\phi_{14}(0) - \xi\phi_{14}(0) \\ \theta\nu_h\phi_{14}(0) - \gamma_a\phi_{15}(0) - \xi\phi_{15}(0) \\ (1-\theta)\nu_h\phi_{14}(0) - \gamma_s\phi_{16}(0) - \xi\phi_{16}(0) \\ (1-p)B_c\frac{\phi_2(-\tau)+\phi_3(-\tau)+\phi_4(-\tau)}{N_f}e^{-\xi\tau} - \xi\phi_{17}(0) \\ pB_c\frac{\phi_2(-\tau)+\phi_3(-\tau)+\phi_4(-\tau)}{N_f}e^{-\xi\tau} + \gamma_a\phi_{15}(0) + \gamma_s\phi_{16}(0) - \alpha\phi_{18}(0) - \xi\phi_{18}(0) \\ \tilde{B}_v(t) - \tilde{\alpha}_v(t)\frac{T_v(0)}{N_h}\phi_{19}(0) - \mu\phi_{19}(0) \\ \tilde{\alpha}_v(t)\frac{T_v(0)}{N_h}\phi_{19}(0) - (\nu_v + \mu)\phi_{20}(0) \\ \nu_v\phi_{20}(0) - \mu\phi_{21}(0) \end{pmatrix},$$

where

$$T_h(0) = \kappa_e\phi_8(0) + \kappa_a\phi_9(0) + \phi_{10}(0) + \kappa_r\phi_{11}(0),$$
$$T_v(0) = \eta_e\big(\phi_2(0) + \phi_8(0) + \phi_{14}(0)\big) + \eta_a\big(\phi_3(0) + \phi_9(0) + \phi_{15}(0)\big) + \phi_4(0) + \phi_{10}(0) + \phi_{16}(0).$$

Notice that $\tilde{f}(t, \phi)$ is continuous in $(t, \phi) \in \mathbb{R}_+ \times \Omega$ and $\tilde{f}(t, \phi)$ is Lipschitz in ϕ on each compact subset of Ω. Therefore, by [37] (Theorems 2.2.1 and 2.2.3) (1) has a unique solution $u(t, \phi)$ on its maximal interval $[0, \sigma_\phi)$ of existence with $u_0 = \phi$.

Let $\phi = (\phi_1, \phi_2, \ldots, \phi_{21}) \in \Omega$. If $\phi_{13} = 0$, then $\tilde{f}_{13}(t,\phi) \geqslant 0$. If $\phi_{17} = 0$, then $\tilde{f}_{17}(t,\phi) \geqslant 0$. If $\phi_{18} = 0$, then $\tilde{f}_{18}(t,\phi) \geqslant 0$. If $\phi_i = 0$ for some $i = \{1,2,\ldots,21\}$, then $\tilde{f}_i(t,\phi) \geqslant 0$. Obviously, the total number of humans, represented by $N_h(t)$, abides by:

$$N_h'(t) = B_c e^{-\xi\tau} - \xi N_c(t) - dN_f(t) - dN_m(t) \geq B_c e^{-\xi\tau} - (\xi + 2d)N_h(t).$$

It is important to note that the linear equation $\frac{dy}{dt} = B_c e^{-\xi\tau} - (\xi + 2d)y(t)$ has a globally stable equilibrium $\frac{B_c e^{-\xi\tau}}{\xi+2d}$ and for any $0 < \delta < \frac{B_c e^{-\xi\tau}}{\xi+2d}$, $\frac{dy}{dt}|_{y=\delta} = B_c e^{-\xi\tau} - (\xi + 2d)\delta > 0$. As a result, if $y(0) \geq \delta$, then $y(t) \geq \delta$ holds true for all $t \geq 0$. Based on the comparison principle, if $N_h(0) = \sum_{i=1}^{18} \phi_i(0) \geq \delta$, then $N_h(t) \geq \delta$. Then by [38] (Theorem 5.2.1 and Remark 5.2.1), the unique solution $u(t,\phi)$ of (1) with $u_0 = \phi$ satisfies $u_t(\phi) \in \Omega$ for all $t \in [0, \sigma_\phi)$.

From (1), we obtain

$$N_h'(t) = B_c e^{-\xi\tau} - \xi N_c(t) - dN_f(t) - dN_m(t) \leq B_c e^{-\xi\tau} - \xi N_h(t), \tag{2}$$

where $\xi \leq d$. Clearly, $N_v(t)$ satisfies

$$N_v'(t) = \tilde{B}_v(t) - \mu N_v(t) \leqslant \hat{\tilde{B}}_v - \mu N_v(t), \ \forall\, t \in [0, \sigma_\phi).$$

Hence, $N_h(t)$ and $N_v(t)$ are ultimately bounded on $[0, \sigma_\phi)$. By [37] (Theorem 2.3.1), it follows that $\sigma_\phi = \infty$. When $N_h(t) > \max\{\frac{B_c e^{-\xi\tau}}{\xi+2d}, \frac{\hat{\tilde{B}}_v}{\mu}\}$ and $N_v(t) > \max\{\frac{B_c e^{-\xi\tau}}{\xi+2d}, \frac{\hat{\tilde{B}}_v}{\mu}\}$, we have

$$\frac{\mathrm{d}N_h(t)}{\mathrm{d}t} < 0 \quad \text{and} \quad \frac{\mathrm{d}N_v(t)}{\mathrm{d}t} < 0.$$

This implies that all solutions are uniformly bounded. □

Next, we investigate the existence and uniqueness of the disease-free periodic solution of system (1). Define

$$\begin{aligned}\psi = \big(&S_f(0), E_f(0), I_f^a(0), I_f^s(0), I_f^r(0), R_f(0), S_m(0), E_m(0), I_m^a(0), I_m^s(0), I_m^r(0), R_m(0), S_c(0), E_c(0),\\ &I_c^a(0), I_c^s(0), M_c(0), R_c(0), S_v(0), E_v(0), I_v(0)\big) \in \mathbb{R}_+^{21}.\end{aligned}$$

When there is no disease present, with a positive initial condition $\psi \in \mathbb{R}_+^{21}$, we have the following system

$$\begin{aligned} S_f'(t) =& \frac{\alpha}{2} S_c(t) - dS_f(t),\\ S_m'(t) =& \frac{\alpha}{2} S_c(t) - dS_m(t),\\ S_c'(t) =& B_c e^{-\xi\tau} - \xi S_c(t) \end{aligned} \tag{3}$$

from the last equation of system (3) we can derive

$$S_c(t) = S_c(0)e^{-\xi t} + \frac{B_c e^{-\xi\tau}}{\xi}(1 - e^{-\xi t}). \tag{4}$$

with an arbitrary initial value $S_c(0)$. Equation (4) has a unique equilibrium $S_c^* = \frac{B_c e^{-\xi\tau}}{\xi}$ in $\mathbb{R}_+$. Consequently, $|S_c(t) - S_c^*| \to 0$ as $t \to \infty$ and S_c^* is globally attractive on $\mathbb{R}_+$. Therefore, system (3) has a unique equilibrium $(S_f^*, S_m^*, S_c^*) = (\frac{\alpha B_c e^{-\xi\tau}}{2d\xi}, \frac{\alpha B_c e^{-\xi\tau}}{2d\xi}, \frac{B_c e^{-\xi\tau}}{\xi})$.

To get the disease-free periodic equilibrium of (1), consider the following equation:

$$\frac{\mathrm{d}S_v(t)}{\mathrm{d}t} = \tilde{B}_v(t) - \mu S_v(t). \tag{5}$$

It is clear that (5) admits a single positive ω-periodic solution $S_v^*(t)$ given by

$$S_v^*(t) = \left[\int_0^t \tilde{B}_v(r)e^{\mu r}dr + \frac{\int_0^\omega \tilde{B}_v(r)e^{\mu r}dr}{e^{\mu t}-1}\right]e^{-\mu},$$

that is globally attractive in $\mathbb{R}$ and, hence, (1) has a single disease-free periodic solution

$$E_0 = \left(S_f^*, 0, 0, 0, 0, 0, S_m^*, 0, 0, 0, 0, 0, S_c^*, 0, 0, 0, 0, 0, S_v^*(t), 0, 0\right). \tag{6}$$

3.1.1. Basic Reproduction Numbers

By linearizing system (1) at the disease-free periodic solution E_0, we get the periodic linear system for the infective variables as follows:

$$\begin{cases} E_f'(t) = \beta T_h(t) + \frac{\tilde{\alpha}_h(t)I_v(t)}{N_h^*}S_f^* - (\nu_h + d)E_f(t), \\ I_f^{a\prime}(t) = \theta\nu_h E_f(t) - \gamma_a I_f^a(t) - dI_f^a(t), \\ I_f^{s\prime}(t) = (1-\theta)\nu_h E_f(t) - \gamma_s I_f^s(t) - dI_f^s(t), \\ I_f^{r\prime}(t) = \gamma_a I_f^a(t) + \gamma_s I_f^s(t) - \gamma_r I_f^r(t) - dI_f^r(t), \end{cases}$$
$$\begin{cases} E_m'(t) = \frac{\tilde{\alpha}_h(t)I_v(t)}{N_h^*}S_m^* - (\nu_h + d)E_m(t), \\ I_m^{a\prime}(t) = \theta\nu_h E_m(t) - \gamma_a I_m^a(t) - dI_m^a(t), \\ I_m^{s\prime}(t) = (1-\theta)\nu_h E_m(t) - \gamma_s I_m^s(t) - dI_m^s(t), \\ I_m^{r\prime}(t) = \gamma_a I_m^a(t) + \gamma_s I_m^s(t) - \gamma_r I_m^r(t) - dI_m^r(t), \end{cases} \tag{7}$$
$$\begin{cases} E_c'(t) = \frac{\tilde{\alpha}_h(t)I_v(t)}{N_h^*}S_c^* - \nu_h E_c(t) - \xi E_c(t), \\ I_c^{a\prime}(t) = \theta\nu_h E_c(t) - \gamma_a I_c^a(t) - \xi I_c^a(t), \\ I_c^{s\prime}(t) = (1-\theta)\nu_h E_c(t) - \gamma_s I_c^s(t) - \xi I_c^s(t), \\ M_c'(t) = (1-p)B_c\frac{E_f(t-\tau)+I_f^a(t-\tau)+I_f^s(t-\tau)}{N_f^*}e^{-\xi\tau} - \xi M_c(t), \end{cases}$$
$$\begin{cases} E_v'(t) = \tilde{\alpha}_v(t)\frac{T_v(t)}{N_h^*}S_v^*(t) - (\nu_v + \mu)E_v(t), \\ I_v'(t) = \nu_v E_v(t) - \mu I_v(t), \end{cases}$$

Let $C := C\left([-\tau, 0], \mathbb{R}^4\right) \times \mathbb{R}^{10}$. Assume that $v = (v_1, v_2, \ldots, v_{14}) : [-\tau, \sigma] \to \mathbb{R}^{14}$ is a continuous function with $\sigma > 0$, we define $v_t \in C$ by

$$v_t(\theta) = (v_1(t+\theta), v_2(t+\theta), v_3(t+\theta), v_4(t+\theta), v_5(t), v_6(t), \ldots, v_{14}(t)),\ \forall\theta \in [-\tau, 0],$$

for any $t \in [0, \sigma)$. Define a map $F : \mathbb{R} \to \mathcal{L}(C, \mathbb{R}^{14})$ and a matrix function $V(t)$ as follows:

$$F(t)\phi = \begin{bmatrix} \beta\left(\kappa_e\phi_8(0) + \kappa_a\phi_9(0) + \phi_{10}(0) + \kappa_r\phi_{11}(0)\right) + \tilde{\alpha}_h(t)\frac{\phi_{14}(0)}{N_h^*}S^* \\ 0 \\ 0 \\ 0 \\ \frac{\tilde{\alpha}_h(t)\phi_{14}(0)}{N_h^*}S_m^* \\ 0 \\ 0 \\ 0 \\ \frac{\tilde{\alpha}_h(t)\phi_{14}(0)}{N_h^*}S_c^* \\ 0 \\ 0 \\ 0 \\ \tilde{\alpha}_v(t)\frac{\eta_e(\phi_2(0)+\phi_8(0)+\phi_{14}(0)) + \eta_a(\phi_3(0)+\phi_9(0)+\phi_{15}(0)) + \phi_4(0)+\phi_{10}(0)+\phi_{16}(0)}{N_h^*}S_v^*(t) \\ 0 \end{bmatrix},$$

$$V(t) = \begin{bmatrix}
\nu_h+d & 0 & 0 & 0 & 0 & 0 & 0 & 0 & 0 & 0 & 0 & 0 & 0 & 0 \\
-\theta\nu_h & \gamma_a+d & 0 & 0 & 0 & 0 & 0 & 0 & 0 & 0 & 0 & 0 & 0 & 0 \\
-(1-\theta)\nu_h & -\gamma_a & \gamma_s+d & 0 & 0 & 0 & 0 & 0 & 0 & 0 & 0 & 0 & 0 & 0 \\
0 & -\gamma_s & -\gamma_s & \gamma_r & 0 & 0 & 0 & 0 & 0 & 0 & 0 & 0 & 0 & 0 \\
0 & 0 & 0 & 0 & \nu_h+d & 0 & 0 & 0 & 0 & 0 & 0 & 0 & 0 & 0 \\
0 & 0 & 0 & 0 & -\theta\nu_h & \gamma_a+d & 0 & 0 & 0 & 0 & 0 & 0 & 0 & 0 \\
0 & 0 & 0 & 0 & -(1-\theta)\nu_h & -\gamma_a & \gamma_s+d & 0 & 0 & 0 & 0 & 0 & 0 & 0 \\
0 & 0 & 0 & 0 & 0 & -\gamma_a & -\gamma_s & \gamma_r & 0 & 0 & 0 & 0 & 0 & 0 \\
0 & 0 & 0 & 0 & 0 & 0 & 0 & 0 & \nu_h+\xi & 0 & 0 & 0 & 0 & 0 \\
0 & 0 & 0 & 0 & 0 & 0 & 0 & 0 & -\theta\nu_h & \gamma_a+\xi & 0 & 0 & 0 & 0 \\
0 & 0 & 0 & 0 & 0 & 0 & 0 & 0 & -(1-\theta)\nu_h & -\gamma_a & \gamma_s+\xi & 0 & 0 & 0 \\
-\frac{(1-p)B_c}{N_f^*} & -\frac{(1-p)B_c}{N_f^*} & -\frac{(1-p)B_c}{N_f^*} & 0 & 0 & 0 & 0 & 0 & 0 & 0 & 0 & \xi & 0 & 0 \\
0 & 0 & 0 & 0 & 0 & 0 & 0 & 0 & 0 & 0 & 0 & 0 & \nu_h+\mu & 0 \\
0 & 0 & 0 & 0 & 0 & 0 & 0 & 0 & 0 & 0 & 0 & 0 & -\nu_h & \mu
\end{bmatrix}.$$

System (7) can be written as:

$$\frac{\mathrm{d}v(t)}{\mathrm{d}t} = F(t)v_t - V(t)v(t),\ \forall \geqslant 0. \tag{8}$$

Assume $Z(t,s), t \geqslant s$ to be the evolution operator of the linear ω-periodic system

$$\frac{\mathrm{d}z}{\mathrm{d}t} = -V(t)z. \tag{9}$$

That is, for each $s \in \mathbb{R}$, the 14×14 matrix $Z(t,s)$ satisfies

$$\frac{\mathrm{d}}{\mathrm{d}t}Z(t,s) = -V(t)Z(t,s), \qquad \forall t \geqslant s,\ Z(s,s) = I,$$

where I is the 14×14 identity matrix.

Following Zhao [39] (Section 2), we suppose that the initial distribution of infectious individuals is $v(t)$, ω-periodic in s. $F(t-s)v_{t-s}$ is the distribution of newly infected individuals at time $t-s$, which is formed by the infectious individuals who were presented throughout the time period $[t-s-\tau, t-s]$ for any $s \geqslant 0$. Then $Z(t,t-s)F(t-s)v_{t-s}$ provides the distribution of those infected individuals who were newly infected at time $t-s$ and remain infected at time t. It concludes that

$$\int_0^\infty Z(t,t-s)F(t-s)v_{t-s}ds = \int_0^\infty Z(t,t-s)F(t-s)v(t-s+.)ds,$$

represents the distribution of accumulative new infections at time t caused by all those infected people raised at a time previous to t.

Let C_ω stands for the ordered Banach space of all ω-periodic functions from $\mathbb{R}$ to $\mathbb{R}^{14}$, that has the maximum norm $\|.\|_\infty$ and the positive cone

$$C_\omega^+ := \{v \in C_\omega : v(t) \geqslant 0,\ \forall t \in \mathbb{R}\}.$$

Then, a linear operator $\mathcal{L} : C_\omega \to C_\omega$ can be defined as

$$[\mathcal{L}v](t) = \int_0^\infty Z(t,t-s)F(t-s)v(t-s+.)ds,\ \forall t \in \mathbb{R},\ v \in C_\omega. \tag{10}$$

As stated in [39], the basic reproduction number is defined as $\mathcal{R}_0 := \rho(\mathcal{L})$. Let $\bar{P}(t)$ be the solution map of (7) for any $t \geqslant 0$ and, hence, $\bar{P}(t)\phi = u_t(\phi)$, where $u(t,\phi)$ is the unique solution of (7) with $u_0 = \phi \in C$. Thus, $\bar{P} := \bar{P}(\omega)$ is the Poincaré map associated with (7). Assume $\rho(\bar{P})$ is the spectral radius of $\bar{P}$. By [39] (Theorem 2.1), we have the following lemma.

Lemma 2. *$\mathcal{R}_0 - 1$ has the same sign as $\rho(\bar{P}) - 1$.*

These results suggest that $\mathcal{R}_0$ is a critical value for the disease local spread, as well as that the stability of the zero solution of system (7) depends on the sign of $\mathcal{R}_0 - 1$.

3.1.2. Derivation of the Time-Average Reproduction Number

In model (1) the delay τ was introduced to take account of the delay between the infection of the mother and the delivery which caused the lag time between the peaks observed on symptomatically infected cases and microcephaly cases. By setting $\tau = 0$, we can use the general approach established in [40] to calculate a formula for the time-average reproduction number $[\mathcal{R}_0]$ of (1).

We calculate a formula for the basic reproduction number $\mathcal{R}_0^A$ of the autonomous model obtained from (1) by setting the time-dependent parameters (mosquito birth $\tilde{B}_v(t) \equiv B_v$) and biting rates ($\tilde{\alpha}_h(t) \equiv \alpha_h$ and $\tilde{\alpha}_v(t) \equiv \alpha_v$) to constant. Given the infectious states E_f, I_f^a, I_f^s, I_f^r, E_m, I_m^a, I_m^s, I_m^r, E_c, I_c^a, I_c^s, E_v and I_v in (1) and substituting the values in

$$\begin{aligned} E_0 &= \left(S_f^*, 0, 0, 0, 0, 0, S_m^*, 0, 0, 0, 0, 0, S_c^*, 0, 0, 0, 0, 0, S_v^*, 0, 0\right) \\ &= \left(\tfrac{\alpha B_c}{2d(\xi+\alpha)}, 0, 0, 0, 0, 0, \tfrac{\alpha B_c}{2d(\xi+\alpha)}, 0, 0, 0, 0, 0, \tfrac{B_c}{\xi+\alpha}, 0, 0, 0, 0, 0, \tfrac{B_v}{\mu}, 0, 0\right), \end{aligned}$$

we compute the matrices F and V for the new infection terms and the remaining transfer terms. These two matrices are, respectively, given by

$$F = \begin{bmatrix} 0 & 0 & 0 & 0 & \beta\kappa_e & \beta\kappa_a & \beta & \beta\kappa_r & 0 & 0 & 0 & 0 & 0 & \frac{\alpha_h S_f^*}{N_h^*} \\ 0 & 0 & 0 & 0 & 0 & 0 & 0 & 0 & 0 & 0 & 0 & 0 & 0 & 0 \\ 0 & 0 & 0 & 0 & 0 & 0 & 0 & 0 & 0 & 0 & 0 & 0 & 0 & 0 \\ 0 & 0 & 0 & 0 & 0 & 0 & 0 & 0 & 0 & 0 & 0 & 0 & 0 & 0 \\ 0 & 0 & 0 & 0 & 0 & 0 & 0 & 0 & 0 & 0 & 0 & 0 & 0 & \frac{\alpha_h S_m^*}{N_h^*} \\ 0 & 0 & 0 & 0 & 0 & 0 & 0 & 0 & 0 & 0 & 0 & 0 & 0 & 0 \\ 0 & 0 & 0 & 0 & 0 & 0 & 0 & 0 & 0 & 0 & 0 & 0 & 0 & 0 \\ 0 & 0 & 0 & 0 & 0 & 0 & 0 & 0 & 0 & 0 & 0 & 0 & 0 & 0 \\ 0 & 0 & 0 & 0 & 0 & 0 & 0 & 0 & 0 & 0 & 0 & 0 & 0 & \frac{\alpha_h S_c^*}{N_h^*} \\ 0 & 0 & 0 & 0 & 0 & 0 & 0 & 0 & 0 & 0 & 0 & 0 & 0 & 0 \\ 0 & 0 & 0 & 0 & 0 & 0 & 0 & 0 & 0 & 0 & 0 & 0 & 0 & 0 \\ 0 & 0 & 0 & 0 & 0 & 0 & 0 & 0 & 0 & 0 & 0 & 0 & 0 & 0 \\ \frac{\alpha_v \eta_e S_v^*}{N_h^*} & \frac{\alpha_v \eta_a S_v^*}{N_h^*} & \frac{\alpha_v S_v^*}{N_h^*} & 0 & \frac{\alpha_v \eta_e S_v^*}{N_h^*} & \frac{\alpha_v \eta_a S_v^*}{N_h^*} & \frac{\alpha_v S_v^*}{N_h^*} & 0 & \frac{\alpha_v \eta_e S_v^*}{N_h^*} & \frac{\alpha_v \eta_a S_v^*}{N_h^*} & \frac{\alpha_v S_v^*}{N_h^*} & 0 & 0 & 0 \\ 0 & 0 & 0 & 0 & 0 & 0 & 0 & 0 & 0 & 0 & 0 & 0 & 0 & 0 \end{bmatrix}$$

and

$$V = \begin{bmatrix} d+\nu_h & 0 & 0 & 0 & 0 & 0 & 0 & 0 & 0 & 0 & 0 & 0 & 0 & 0 \\ -\theta\nu_h & \gamma_a+d & 0 & 0 & 0 & 0 & 0 & 0 & 0 & 0 & 0 & 0 & 0 & 0 \\ -(1-\theta)\nu_h & 0 & \gamma_s+d & 0 & 0 & 0 & 0 & 0 & 0 & 0 & 0 & 0 & 0 & 0 \\ 0 & -\gamma_a & -\gamma_s & \gamma_r+d & 0 & 0 & 0 & 0 & 0 & 0 & 0 & 0 & 0 & 0 \\ 0 & 0 & 0 & 0 & d+\nu_h & 0 & 0 & 0 & 0 & 0 & 0 & 0 & 0 & 0 \\ 0 & 0 & 0 & 0 & -\theta\nu_h & \gamma_a+d & 0 & 0 & 0 & 0 & 0 & 0 & 0 & 0 \\ 0 & 0 & 0 & 0 & -(1-\theta)\nu_h & 0 & \gamma_s+d & 0 & 0 & 0 & 0 & 0 & 0 & 0 \\ 0 & 0 & 0 & 0 & 0 & -\gamma_a & -\gamma_s & \gamma_r+d & 0 & 0 & 0 & 0 & 0 & 0 \\ 0 & 0 & 0 & 0 & 0 & 0 & 0 & 0 & \xi+\nu_h & 0 & 0 & 0 & 0 & 0 \\ 0 & 0 & 0 & 0 & 0 & 0 & 0 & 0 & -\theta\nu_h & \gamma_a+\xi & 0 & 0 & 0 & 0 \\ 0 & 0 & 0 & 0 & 0 & 0 & 0 & 0 & -(1-\theta)\nu_h & 0 & \gamma_s+\xi & 0 & 0 & 0 \\ \frac{(p-1)B_c}{N_f^*} & \frac{(p-1)B_c}{N_f^*} & \frac{(p-1)B_c}{N_f^*} & 0 & 0 & 0 & 0 & 0 & 0 & 0 & 0 & \xi & 0 & 0 \\ 0 & 0 & 0 & 0 & 0 & 0 & 0 & 0 & 0 & 0 & 0 & 0 & \mu+\nu_v & 0 \\ 0 & 0 & 0 & 0 & 0 & 0 & 0 & 0 & 0 & 0 & 0 & 0 & -\nu_v & \mu \end{bmatrix},$$

hence the next generation matrix FV^{-1} has the following characteristic polynomial:

$$\lambda^{11}\left(\lambda^3 - (R_{fv}R_{vf} + R_{vm}R_{mv} + R_{vc}R_{cv})\lambda - R_{mf}R_{fv}R_{vm}\right) = 0$$

where

$$
\begin{aligned}
R_{mf} &= \frac{\beta\kappa_e}{d+\nu_h} + \frac{\theta\beta\kappa_a\nu_h}{(d+\gamma_a)(d+\nu_h)} + \frac{(1-\theta)\beta\nu_h}{(d+\gamma_s)(d+\nu_h)} + \frac{\beta\kappa_r\nu_h(\gamma_a\gamma_s+\theta\gamma_a d+(1-\theta)\gamma_s d)}{(d+\gamma_a)(d+\gamma_s)(d+\gamma_r)(d+\nu_h)} \\
R_{fv} &= R_{mv} = \frac{\alpha_v\eta_e S_v^*}{(d+\nu_h)N_h^*} + \frac{\theta\alpha_v\eta_a\nu_h S_v^*}{(d+\gamma_a)(d+\nu_h)N_h^*} + \frac{(1-\theta)\alpha_v\nu_h S_v^*}{(d+\gamma_a)(d+\nu_h)N_h^*}, \\
R_{cv} &= \frac{\alpha_v\eta_e S_v^*}{(\xi+\nu_h)N_h^*} + \frac{\theta\alpha_v\eta_a\nu_h S_v^*}{(\xi+\gamma_a)(\xi+\nu_h)N_h^*} + \frac{(1-\theta)\alpha_v\nu_h S_v^*}{(\xi+\gamma_s)(\xi+\nu_h)N_h^*}, \\
R_{vf} &= R_{vm} = \frac{\alpha}{2d}R_{vc} = \frac{\alpha}{2d}\frac{\alpha_h\nu_v B_c}{\mu(\xi+\alpha)(\mu+\nu_v)N_h^*},
\end{aligned}
$$

The characteristic polynomial, therefore, takes the form

$$2d\lambda^3 - 2R_{vc}(dR_{cv} + \alpha R_{fv})\lambda - \alpha R_{mf}R_{fv}R_{vc} = 0.$$

Following [40], $\mathcal{R}_0^A$ is the spectral radius of FV^{-1}. Accordingly, $\mathcal{R}_0^A$ corresponds to the dominant eigenvalue given by the root of the cubic equation

$$
\begin{aligned}
\mathcal{R}_0^A = {} & \frac{2R_{vc}\left(dR_{cv}+\alpha R_{fv}\right)}{3\sqrt[3]{6}\left(\sqrt{(9d^2\alpha R_{fv}R_{mf}R_{cv})^2-48R_{vc}^3\left(dR_{cv}+\alpha R_{fv}\right)^3}-9d^2\alpha R_{fv}R_{mf}R_{cv}\right)^{1/3}} \\
& + \frac{\left(\sqrt{(9d^2\alpha R_{fv}R_{mf}R_{cv})^2-48R_{vc}^3\left(dR_{cv}+\alpha R_{fv}\right)^3}-9d^2\alpha R_{fv}R_{mf}R_{cv}\right)^{1/3}}{3\sqrt[3]{36}d},
\end{aligned}
\tag{11}
$$

where R_{mf} is the basic reproduction number corresponding to sexual transmission and R_{fv}, R_{cv}, R_{vc} are the reproductive numbers relevant to vector-borne transmission.

We derive the formula for $[\mathcal{R}_0]$ (the time-average reproduction number) of the corresponding non-autonomous model (1) by using the following remark presented in [36].

Remark 1. *Given a continuous ω-periodic function $q(t)$, its average is defined as*

$$[q] := \frac{1}{\omega}\int_0^\omega q(t)\,dt.$$

Then, $[\mathcal{R}_0]$ is given by

$$
\begin{aligned}
[\mathcal{R}_0] = {} & \frac{2[R_{vc}]\left(d[R_{cv}]+\alpha[R_{fv}]\right)}{3\sqrt[3]{6}\left(\sqrt{(9d^2\alpha[R_{fv}]R_{mf}[R_{cv}])^2-48[R_{vc}]^3\left(d[R_{cv}]+\alpha[R_{fv}]\right)^3}-9d^2\alpha[R_{fv}]R_{mf}[R_{cv}]\right)^{\frac{1}{3}}} \\
& + \frac{\left(\sqrt{(9d^2\alpha[R_{fv}]R_{mf}[R_{cv}])^2-48[R_{vc}]^3\left(d[R_{cv}]+\alpha[R_{fv}]\right)^3}-9d^2\alpha[R_{fv}]R_{mf}[R_{cv}]\right)^{\frac{1}{3}}}{3\sqrt[3]{36}d},
\end{aligned}
\tag{12}
$$

where

$$
\begin{aligned}
[R_{fv}] &= \frac{\eta_e[\tilde{\alpha}_v][\tilde{B}_v]}{\mu(d+\nu_h)N_h^*} + \frac{\theta\eta_a\nu_h[\tilde{\alpha}_v][\tilde{B}_v]}{\mu(d+\gamma_a)(d+\nu_h)N_h^*} + \frac{(1-\theta)\nu_h[\tilde{\alpha}_v][\tilde{B}_v]}{\mu(d+\gamma_a)(d+\nu_h)N_h^*}, \\
[R_{cv}] &= \frac{\eta_e[\tilde{\alpha}_v][\tilde{B}_v]}{\mu(\xi+\nu_h)N_h^*} + \frac{\theta\eta_a\nu_h[\tilde{\alpha}_v][\tilde{B}_v]}{\mu(\xi+\gamma_a)(\xi+\nu_h)N_h^*} + \frac{(1-\theta)\nu_h[\tilde{\alpha}_v][\tilde{B}_v]}{\mu(\xi+\gamma_a)(\xi+\nu_h)N_h^*}, \\
[R_{vc}] &= \frac{B_c\nu_v[\tilde{\alpha}_h]}{\mu(\xi+\alpha)(\mu+\nu_v)N_h^*}.
\end{aligned}
$$

3.1.3. Global Dynamics

In terms of $\mathcal{R}_0$, we investigate the global dynamics of (1). We employ the theory of monotone semiflows developed in [41] (Section 2.3). Then, we continue with a new phase space on which (7) eventually forms a strongly monotone periodic semiflow. We prove that, if $\mathcal{R}_0 < 1$, then the unique disease-free equilibrium is globally asymptotically stable and the disease dies out, while, if $\mathcal{R}_0 > 1$, the infection persists and there exists at least an ω-periodic solution of (1).

Define

$$Y := C\big([-\tau, 0], \mathbb{R}^4\big) \times \mathbb{R}^{10} \text{ and } Y_+ := C\big([-\tau, 0], \mathbb{R}^4_+\big) \times \mathbb{R}^{10}_+.$$

The following lemma can be obtained by using the method of steps.

Lemma 3. *For any $\phi \in Y_+$ and for all $t \geqslant 0$, system (7) has a unique non-negative solution $v(t, \phi)$ with $v_0 = \phi$.*

Assume that $P(t)$ is the solution map of system (1) on Y for any given $t \geqslant 0$. Therefore, $P := P(\omega)$ is the Poincaré map corresponding to the linear Equation (7) and $\rho(\bar{P}) = \rho(P)$ by using Lou and Zhao [42] (Lemma 3.8).

Define

$$\begin{aligned} X &:= C([-\tau, 0], \mathbb{R}^6_+) \times \mathbb{R}^{15}_+, \\ X_0 &:= \{\phi = (\phi_1, \phi_2, \ldots, \phi_{21}) \in X : \phi_i(0) > 0,\ i = 2, 3, 4, 5, 8, 9, 10, 11, 14, 15, 16, 20, 21\}, \\ \partial X_0 &:= X \setminus X_0 = \{\phi \in X : \phi_i(0) = 0,\ i = 2, 3, 4, 5, 8, 9, 10, 11, 14, 15, 16, 20, 21\}. \end{aligned}$$

Theorem 1. *The subsequent statements are valid:*

(i) *If $\rho(P) < 1$, the disease-free periodic solution E_0 defined by (6) is globally attractive for system (1) in X.*

(ii) *If $\rho(P) > 1$, then system (1) admits a positive ω-periodic solution and there exists a positive constant $\kappa > 0$ such that any solution $u(t, \phi)$ of system (1) for all initial values $\phi \in X_0$ satisfies*

$$\begin{aligned} \liminf_{t\to\infty} \Big(& E_f(t,\phi), I_f^a(t,\phi), I_f^s(t,\phi), I_f^r(t,\phi), E_m(t,\phi), I_m^a(t,\phi), I_m^s(t,\phi), I_m^r(t,\phi), E_c(t,\phi), \\ & I_c^a(t,\phi), I_c^s(t,\phi), E_v(t,\phi), I_v(t,\phi) \Big)^T \geqslant (\kappa, \kappa, \kappa, \kappa, \kappa, \kappa, \kappa, \kappa, \kappa, \kappa, \kappa, \kappa, \kappa)^T. \end{aligned}$$

Proof. If $\rho(P) < 1$, let $v(t, \phi)$ and $w(t, \psi)$ be the unique solutions of (7) with $v_0 = \phi$ and $w_0 = \psi$, respectively, for any ψ and ϕ in Y_+ with $\phi \geqslant \psi$. Smith [38] (Theorem 5.1.1) implies that $v(t, \phi) \geqslant v(t, \psi)$ for all $t \geqslant 0$ and. hence, $P : Y_+ \to Y_+$ is monotone for all $t \geqslant 0$. Consider $\phi, \psi \in Y$ satisfy $\phi > \psi$ and represent $v(t, \phi) = (\bar{x}_1(t), \bar{x}_2(t), \ldots, \bar{x}_{14}(t))$ and $w(t, \psi) = (x_1(t), x_2(t), \ldots, x_{14}(t))$. By applying a simple comparison argument on each interval $[n\tau, (n+1)\tau], n \in \mathbb{N}$, it is possible to demonstrate that $\bar{x}_i(t) > x_i(t)$ for all $t > t_0, i = \{1, 2, 3, 4\}$. The next step is to demonstrate that $P(t)$ becomes eventually strongly monotone. We assume, without losing generality, that $\phi_{14} > \psi_{14}$.

Claim 1. There exists $t_0 \in [0, \tau]$ s.t. $\bar{x}_1(t) > x_1(t), \forall\, t \geqslant t_0$.
First, for some $t_0 \in [0, \tau]$, we show that $\bar{x}_1(t_0) > x_1(t_0)$. If not, then for each $t_0 \in [0, \tau]$, $\bar{x}_1(t) = x_1(t)$ and, consequently, $\frac{\mathrm{d}\bar{x}_1(t)}{\mathrm{d}t} = \frac{\mathrm{d}x_1(t)}{\mathrm{d}t}$ for all $t_0 \in (0, \tau)$. Then, we get

$$\tilde{\alpha}_h(t) \frac{S_f^*}{N_h^*} (\bar{x}_{14}(t) - x_{14}(t)) - (\nu_h + d)(\bar{x}_1(t) - x_1(t)) = 0.$$

It is observed that $\bar{x}_1(t) = x_1(t)$ and $\bar{x}_{14}(t) = x_{14}(t)$ for all $t_0 \in [0, \tau]$, then $\phi_{14}(\theta) = \psi_{14}(\theta)$ for all $t_0 \in [0, \tau]$, which contradicts the hypothesis that $\phi_{14} > \psi_{14}$.

Let $g_1(t,x) := \tilde{\alpha}_h(t)\frac{S_f^*}{N_h^*}x_{14}(t) - (\nu_h + d)x(t)$. Then, we have

$$\begin{aligned}\frac{\mathrm{d}\bar{x}_1(t)}{\mathrm{d}t} &= \tilde{\alpha}_h(t)\frac{S_f^*}{N_h^*}\bar{x}_{14}(t) - (\nu_h + d)\bar{x}_1(t)\\ &\geqslant \tilde{\alpha}_h(t)\frac{S_f^*}{N_h^*}x_{14}(t) - (\nu_h + d)\bar{x}_1(t)\\ &= g_1(t,\bar{x}_1(t)),\end{aligned}$$

we obtain $\frac{\mathrm{d}\bar{x}_1(t)}{\mathrm{d}t} - g_1(t,\bar{x}_1(t)) \geqslant 0 = \frac{\mathrm{d}x_1(t)}{\mathrm{d}t} - g_1(t,x_1(t))\ \forall t \geqslant t_0$. Since $\bar{x}_1(t_0) > x_1(t_0)$, the comparison theorem [43] (Theorem 4) indicates that $\bar{x}_1(t) > x_1(t), \forall\, t \geqslant t_0$.

Claim 2. $\bar{x}_2(t) > x_2(t), \forall\, t \geqslant t_0 + \tau$.
Let $g_2(t,x) := \theta\nu_h x_1(t) - (\gamma_a + d)x(t)$. Then we have

$$\begin{aligned}\frac{\mathrm{d}\bar{x}_2(t)}{\mathrm{d}t} &= \theta\nu_h\bar{x}_1(t) - (\gamma_a + d)\bar{x}_2(t)\\ &\geqslant \theta\nu_h x_1(t) - (\gamma_a + d)\bar{x}_2(t)\\ &= g_2(t,\bar{x}_2(t)),\end{aligned}$$

and, hence, $\frac{\mathrm{d}\bar{x}_2(t)}{\mathrm{d}t} - g_2(t,\bar{x}_2(t)) \geqslant 0 = \frac{\mathrm{d}x_2(t)}{\mathrm{d}t} - g_2(t,x_2(t))\ \forall t > t_0$. It follows from [43] (Theorem 4) that $\bar{x}_2(t) > x_2(t)$ for all $t > t_0 + \tau$.

Claim 3. $\bar{x}_3(t) > x_3(t)$ for all $t \geqslant t_0$.
Let $g_3(t,x) := (1-\theta)\nu_h x_1(t) - (\gamma_s + d)x(t)$, Then we have

$$\begin{aligned}\frac{\mathrm{d}\bar{x}_3}{\mathrm{d}t} &= (1-\theta)\nu_h\bar{x}_1(t) - (\gamma_s + d)\bar{x}_3(t)\\ &\geqslant (1-\theta)\nu_h x_1(t) - (\gamma_s + d)\bar{x}_3(t)\\ &= g_3(t,\bar{x}_3(t)),\end{aligned}$$

and hence, $\frac{\mathrm{d}\bar{x}_3(t)}{\mathrm{d}t} - g_3(t,\bar{x}_3(t)) \geqslant 0 = \frac{\mathrm{d}x_3(t)}{\mathrm{d}t} - g_3(t,x_3(t))\ \forall t > t_0$. It follows from [43] (Theorem 4) that $\bar{x}_3(t) > x_3(t)$ for all $t > t_0$.

Claim 4. $\bar{x}_4(t) > x_4(t)$ for all $t \geqslant t_0$.
Let $g_4(t,x) := \gamma_a x_2(t) + \gamma_s x_3(t) - (\gamma_r + d)x(t)$. Then we have

$$\begin{aligned}\frac{\mathrm{d}\bar{x}_4}{\mathrm{d}t} &= \gamma_a\bar{x}_2(t) + \gamma_s\bar{x}_3(t) - (\gamma_r + d)\bar{x}_4(t)\\ &\geqslant \gamma_a x_2(t) + \gamma_s x_3(t) - (\gamma_r + d)\bar{x}_4(t)\\ &= g_4(t,\bar{x}_4(t)),\end{aligned}$$

and therefore, $\frac{\mathrm{d}\bar{x}_3(t)}{\mathrm{d}t} - g_3(t,\bar{x}_3(t)) \geqslant 0 = \frac{\mathrm{d}x_3(t)}{\mathrm{d}t} - g_3(t,x_3(t))\ \forall t > t_0$. It follows from [43] (Theorem 4) that $\bar{x}_3(t) > x_3(t)$ for all $t > t_0$.

Claim *i* $(i = 5,6,\ldots,14)$**.** $\bar{x}_i(t) > x_i(t)$, $i = 5,6,\ldots,14$ for all $t \geqslant t_0$.
In a similar way to the previous four claims, we can show that $\bar{x}_i(t) > x_i(t)$, $i = 5,6,\ldots,14$ for all $t \geqslant t_0$.

Given two positive real numbers a and b, we write $a \gg b$ if and only if a is much greater than b. If we take into consideration the claims made above, we arrive at

$$\big(\bar{x}_1(t),\bar{x}_2(t),\ldots,\bar{x}_{14}(t)\big) \gg \big(x_1(t),x_2(t),\ldots,x_{14}(t)\big), \quad \forall t > t_0 + \tau.$$

Because $t_0 \in [0,\tau]$, it can be shown that

$$\big(\bar{x}_{1t},\bar{x}_{2t},\ldots,\bar{x}_{14t}\big) \gg \big(x_{1t},x_{2t},\ldots,x_{14t}\big), \quad \forall t > 2\tau,$$

that is $v_t(\phi) \gg w_t(\psi)$ for all $t > 2\tau$. Hence, it follows that $P(t)$ is strongly monotone for any $t > 2\tau$.

According to [37] (Theorem 3.6.1), the linear operator $\bar{P}(t)$ is compact on Y_+ for any $t \geqslant 2\tau$. Hence, $P(t)$ is compact and strongly monotone on Y for $t \geqslant 2\tau$. Select a positive integer $n_0 > 0$ such that $n_0\omega > 2\tau$. Given that $P^{n_0\omega} = P(n_0\omega)$, it follows from [44] (Lemma 3.1) that $\rho(P)$ is a simple eigenvalue of P with a strongly positive eigenvector and the modulus of any additional eigenvalue is smaller than $\rho(P)$. By [45] (Lemma 1), there is a positive ω-periodic function $\bar{v}(t) = (\bar{v}_1(t), \bar{v}_2(t), \ldots, \bar{v}_{14}(t))^T$ s.t. $v^*(t) = e^{\lambda t}\bar{v}(t)$ is a positive solution of (7) where $\lambda = \frac{\ln \rho(P)}{\omega}$.

Assume the linear periodic system with parameter ϵ:

$$
\begin{aligned}
E_f'(t) &= \beta T_h(t) + \tilde{\alpha}_h(t) I_v(t) \frac{S_f^*}{N_h^* - \epsilon} - (\nu_h + d) E_f(t),\\
I_f^{a\prime}(t) &= \theta \nu_h E_f(t) - \gamma_a I_f^a(t) - d I_f^a(t),\\
I_f^{s\prime}(t) &= (1-\theta)\nu_h E_f(t) - \gamma_s I_f^s(t) - d I_f^s(t),\\
I_f^{r\prime}(t) &= \gamma_a I_f^a(t) + \gamma_s I_f^s(t) - \gamma_r I_f^r(t) - d I_f^r(t),\\
E_m'(t) &= \tilde{\alpha}_h(t) I_v(t) \frac{S_m^*}{N_h^* - \epsilon} - (\nu_h + d) E_m(t),\\
I_m^{a\prime}(t) &= \theta \nu_h E_m(t) - \gamma_a I_m^a(t) - d I_m^a(t),\\
I_m^{s\prime}(t) &= (1-\theta)\nu_h E_m(t) - \gamma_s I_m^s(t) - d I_m^s(t),\\
I_m^{r\prime}(t) &= \gamma_a I_m^a(t) + \gamma_s I_m^s(t) - \gamma_r I_m^r(t) - d I_m^r(t),\\
E_c'(t) &= \tilde{\alpha}_h(t) I_v(t) \frac{S_c^*}{N_h^* - \epsilon} - \nu_h E_c(t) - \xi E_c(t),\\
I_c^{a\prime}(t) &= \theta \nu_h E_c(t) - \gamma_a I_c^a(t) - \xi I_c^a(t),\\
I_c^{s\prime}(t) &= (1-\theta)\nu_h E_c(t) - \gamma_s I_c^s(t) - \xi I_c^s(t),\\
M_c'(t) &= (1-p) B_c \frac{E_f(t-\tau) + I_f^a(t-\tau) + I_f^s(t-\tau)}{N_f^* - \epsilon} e^{-\xi\tau} - \xi M_c(t),\\
E_v'(t) &= \tilde{\alpha}_v(t) T_v(t) \frac{S_v^*(t) + \epsilon}{N_h^* - \epsilon} - (\nu_v + \mu) E_v(t),\\
I_v'(t) &= \nu_v E_v(t) - \mu I_v(t).
\end{aligned}
\tag{13}
$$

Assume that $P_\epsilon(t)$ is the solution map of system (13) on Y_+ and $P_\epsilon := P_\epsilon(\omega)$. Since $\lim_{\epsilon\to 0} \rho(P_\epsilon) = \rho(P) < 1$, we can choose a small enough $\epsilon > 0$ s.t. $\rho(P_\epsilon) < 1$. It is straightforward to demonstrate that $P_\epsilon(t)$ is also compact and eventually strongly monotone on Y. Then, there exists a positive ω-periodic function $v_\epsilon(t) = (v_{\epsilon_1}(t), v_{\epsilon_2}(t), \ldots, v_{\epsilon_{14}}(t))$ such that $u_\epsilon(t) = e^{\frac{\ln \rho(P_\epsilon)}{\omega} t} v_\epsilon(t)$ is a positive solution of (13). As a result,

$$\lim_{t\to\infty} u_\epsilon(t) = 0.$$

Clearly, $S_v(t)$ satisfies $S_v'(t) = \tilde{B}_v(t) - \mu S_v(t)$; it has a globally attractive ω-periodic solution $S_v^*(t)$. Then there is a large enough integer $T_1 > 0$ s.t. $T_1\omega > \tau$ and $S_v^*(t) - \epsilon \leqslant S_v(t) \leqslant S_v^*(t) + \epsilon$ for all $t \geqslant T_1\omega$. Then we have

$$
\begin{aligned}
E_f'(t) &\leq \beta T_h(t) + \tilde{\alpha}_h(t) I_v(t) \frac{S_f^*}{N_h^* - \epsilon} - (\nu_h + d) E_f(t),\\
I_f^{a\prime}(t) &\leq \theta \nu_h E_f(t) - \gamma_a I_f^a(t) - d I_f^a(t),\\
I_f^{s\prime}(t) &\leq (1-\theta)\nu_h E_f(t) - \gamma_s I_f^s(t) - d I_f^s(t),
\end{aligned}
$$

$$
\begin{aligned}
I_f^{r\prime}(t) &\leq \gamma_a I_f^a(t) + \gamma_s I_f^s(t) - \gamma_r I_f^r(t) - d I_f^r(t),\\
E_m'(t) &\leq \tilde{\alpha}_h(t) I_v(t) \frac{S_m^*}{N_h^* - \epsilon} - (\nu_h + d) E_m(t),\\
I_m^{a\prime}(t) &\leq \theta \nu_h E_m(t) - \gamma_a I_m^a(t) - d I_m^a(t),\\
I_m^{s\prime}(t) &\leq (1-\theta)\nu_h E_m(t) - \gamma_s I_m^s(t) - d I_m^s(t),\\
I_m^{r\prime}(t) &\leq \gamma_a I_m^a(t) + \gamma_s I_m^s(t) - \gamma_r I_m^r(t) - d I_m^r(t),\\
E_c'(t) &\leq \tilde{\alpha}_h(t) I_v(t) \frac{S_c^*}{N_h^* - \epsilon} - \nu_h E_c(t) - \xi E_c(t),\\
I_c^{a\prime}(t) &\leq \theta \nu_h E_c(t) - \gamma_a I_c^a(t) - \xi I_c^a(t),\\
I_c^{s\prime}(t) &\leq (1-\theta)\nu_h E_c(t) - \gamma_s I_c^s(t) - \xi I_c^s(t),\\
M_c'(t) &\leq (1-p) B_c \frac{E_f(t-\tau) + I_f^a(t-\tau) + I_f^s(t-\tau)}{N_f^* - \epsilon} e^{-\xi\tau} - \xi M_c(t),\\
E_v'(t) &\leq \tilde{\alpha}_v(t) T_v(t) \frac{S_v^*(t) + \epsilon}{N_h^* - \epsilon} - (\nu_v + \mu) E_v(t),\\
I_v'(t) &\leq \nu_v E_v(t) - \mu I_v(t),
\end{aligned}
$$

for all $t \geqslant T_1\omega$. Choose a sufficiently large number $K > 0$ such that

$$
\begin{aligned}
&\big(E_f(t,\phi), I_f^a(t,\phi), I_f^s(t,\phi), I_f^r(t,\phi), E_m(t,\phi), I_m^a(t,\phi), I_m^s(t,\phi), I_m^r(t,\phi), E_c(t,\phi), I_c^a(t,\phi), I_c^s(t,\phi),\\
&\qquad E_v(t,\phi), I_v(t,\phi)\big) \leqslant K u_\epsilon(t),
\end{aligned}
$$

for all $t \in [T_1\omega, T_1\omega + \tau]$. By using [38] (Theorem 5.1.1), $\forall\, t \geqslant T_1\omega + \tau$, we obtain

$$
\begin{aligned}
\lim_{t\to\infty} &\big(E_f(t,\phi), I_f^a(t,\phi), I_f^s(t,\phi), I_f^r(t,\phi), E_m(t,\phi), I_m^a(t,\phi), I_m^s(t,\phi), I_m^r(t,\phi), E_c(t,\phi), I_c^a(t,\phi),\\
&I_c^s(t,\phi), E_v(t,\phi), I_v(t,\phi)\big)^T = (0,0,0,0,0,0,0,0,0,0,0,0,0,0)^T.
\end{aligned}
$$

Furthermore, it follows from the chain transitive sets arguments (see, [46] (Theorem 3.6) and [47] (Theorem 2.5)) that $\lim_{t\to\infty}(S_f(t) - S_f^*) = 0$, $\lim_{t\to\infty} R_f(t) = 0$, $\lim_{t\to\infty}(S_m(t) - S_m^*) = 0$, $\lim_{t\to\infty} R_m(t) = 0$, $\lim_{t\to\infty}(S_c(t) - S_c^*) = 0$, $\lim_{t\to\infty} R_c(t) = 0$ and $\lim_{t\to\infty}(S_v(t) - S_v^*(t)) = 0$. This completes the proof of the first statement.

For the sake of simplicity, we only show the main steps of the proof of the second statement when $\rho(P) > 1$. In this case, we employ the persistence theory for periodic semiflows.

Let $Q(t)\colon X \to X$ be the solution maps of (1) on X, that is, $Q(t)\psi = u_t(\phi)$, $t \geqslant 0$, where $u(t,\phi)$ is the unique solution of (1) satisfying $u_0 = \phi \in X$. Therefore, $Q := Q(\omega)$ is the Poincaré map associated with (1). From (1), it follows that $Q(t)X_0 \subseteq X_0$ for all $t \geqslant 0$. It is important to note that a map Q is point dissipative if there exists a bounded set B such that, for each $x \in \mathbb{R}^n$, there is an integer $n_0 = n_0(x)$ such that $Q^n x \in B$ for $n \geq n_0$. Therefore, the discrete-time system $\{Q^n\colon X \to X\}_{n\geqslant 0}$ is point dissipative by Lemma 1 and from [37] (Theorem 3.6.1), $Q(t)$ is compact for each $t \geqslant \tau$, and, then, Q^n is compact for enough large n. According to [39] (Theorem 1.1.3), Q has a global attractor.

Next, we demonstrate that Q is uniformly persistent w.r.t. $(X_0, \partial X_0)$. Let $M = \big(S_f^*, 0,0,0,0,0, S_m^*, 0,0,0,0,0, S_c^*, 0,0,0,0,0, S_v^*, 0, 0\big)$, where $S_v^* = S_v^*(\xi)$ for all $\xi \in [-\tau, 0]$. Define

$$
\begin{aligned}
M_\partial &:= \{\phi \in \partial X_0 : Q^n(\phi) \in \partial X_0,\ \forall n \geqslant 0\}\\
&= \{\phi \in \partial X_0 : \phi_i(0) = 0,\ i = 2,3,4,5,8,9,10,11,14,15,16,20,21\}.
\end{aligned}
$$

For any given $\phi \in M_\partial$, we see that $Q^n(\phi) \to M$ as $n \to \infty$ by using the theory of internally chain transitive sets (see [39] (Theorems 1.2.1 and 1.2.2) and [42]). From the above discussion, it is clear that M is an isolated invariant set for Q in X, and $W^s(M) \bigcap X_0 = \emptyset$,

where $W^s(M)$ is the stable set of M for Q. By the acyclicity theory on uniform persistence for maps (see [39] (Theorem 1.3.1 and Remark 1.3.1)), it follows that $Q : X \to X$ is uniformly persistent w.r.t. $(X_0, \partial X_0)$ where there exists $\kappa_0 > 0$ s.t.

$$\liminf_{n\to\infty} d(Q^n(\phi), \partial X_0) \geqslant \kappa_0, \ \forall \phi \in X_0.$$

As a result, $Q : X_0 \to X_0$ has a compact global attractor A_0 by [39] (Theorem 4.5). For any $\phi \in A_0$, we have $\phi_i(0) > 0$ for all $i = \{2, 3, 4, 5, 8, 9, 10, 11, 14, 15, 16, 20, 21\}$. Let $B_0 := \bigcup_{t\in[0,\omega]} Q(t)A_0$. Then $\phi_i(0) > 0$, $i = \{2, 3, 4, 5, 8, 9, 10, 11, 14, 15, 16, 20, 21\}$, for all $\phi \in B_0$. Furthermore, $B_0 \subseteq X_0$ and $\lim_{t\to\infty} d(Q(t)\phi, B_0) = 0$ for all $\phi \in X_0$. The attractiveness of B_0 completes the proof. □

Following the statements in [48] (Lemma 3.8), we get $\rho(P) = \rho(\bar{P})$. Using Lemma 2 and Theorem 1, we have the subsequent result.

Theorem 2. *The following statements are valid:*

1. *If $\mathcal{R}_0 < 1$, then the disease-free periodic solution E_0 defined by (6) is globally attractive for system (1) in X.*
2. *If $\mathcal{R}_0 > 1$, then system (1) admits a positive ω-periodic solution and there exists a positive constant $\kappa > 0$ such that any solution $u(t, \phi)$ of system (1) for all initial values $\phi \in X_0$ satisfies*

$$\liminf_{t\to\infty} \left(E_f(t,\phi), I_f^a(t,\phi), I_f^s(t,\phi), I_f^r(t,\phi), E_m(t,\phi), I_m^a(t,\phi), I_m^s(t,\phi), I_m^r(t,\phi), E_c(t,\phi), I_c^a(t,\phi), I_c^s(t,\phi), E_v(t,\phi), I_v(t,\phi)\right)^T \geqslant (\kappa,\kappa,\kappa,\kappa,\kappa,\kappa,\kappa,\kappa,\kappa,\kappa,\kappa,\kappa,\kappa)^T.$$

3.2. Numerical Results

Figure 3a is in accordance with the analytical results noting that the disease-free equilibrium E_0 is globally asymptotically stable if $\mathcal{R}_0 < 1$. According to Theorem 1, Equation (1) is persistent w.r.t. the infective compartments if $\mathcal{R}_0 > 1$. Figure 3b indicates the disease persistence if $\mathcal{R}_0 > 1$.

3.2.1. Parameter Estimation for Colombia

By employing the method explained in Section 2.3, we fitted our system to symptomatically infected and microcephaly data in Colombia, 2015–17. Figure 2 shows the weekly confirmed ZIKV cases of the 2015–2017 outbreak and the weekly microcephaly cases of 2015–2017 from Colombia with parameter values are given in Table 2. Figure 4a depicts model (1) fitted to symptomatically infected data and Figure 4b illustrates model (1) fitted to microcephaly data from Colombia, showing a reasonably good fit.

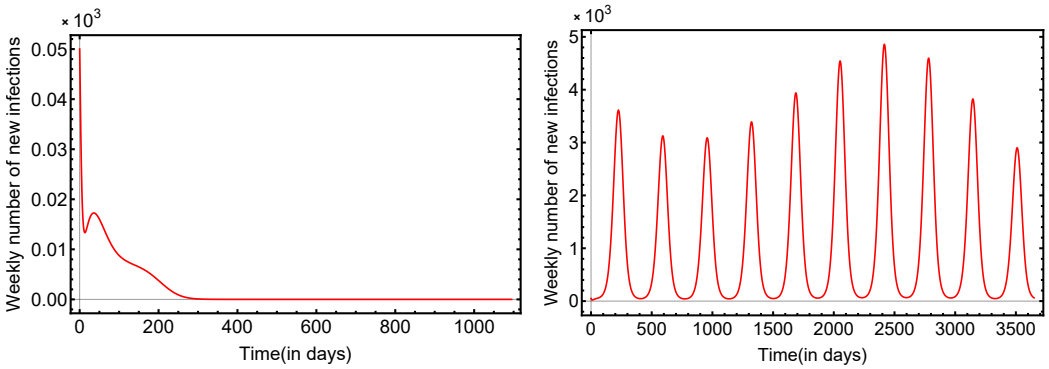

(a) $\mathcal{R}_0 = 0.585 < 1$ **(b)** $\mathcal{R}_0 = 1.2 > 1$

Figure 3. Weekly number of Zika new infections in (**a**) when $\mathcal{R}_0 = 0.585 < 1$, $\alpha_h = 0.112$, $\alpha_v = 1.2$ and $B_v = 41,400$, and in (**b**) when $\mathcal{R}_0 = 1.2 > 1$, $\alpha_h = 0.185$, $\alpha_v = 0.139$ and $B_v = 95,000$. The rest of the parameter values are given in Table 2.

Table 2. Parameters, ranges and fitted values of model (1) in the case of Colombia.

Parameter	Range	Value Symptomatically Infected	Value Microcephaly	Source
B_c	–	1826.81	1826.81	[49]
ξ	$\frac{1}{22\times365}-\frac{1}{14\times365}$	$\frac{1}{16.98\times365}$	$\frac{1}{18.68\times365}$	[23]
d	–	0.0000368	0.0000368	[49]
α	$\frac{1}{18\times365}-\frac{1}{12\times365}$	$\frac{1}{16.52\times365}$	$\frac{1}{17.56\times365}$	[23]
β	0.01–0.1	0.029	0.029	[14,24]
α_h	0.03–0.75	0.382	0.283	[50,51]
α_v	0.09–0.75	0.227	0.227	[50,51]
θ	0.75–0.9	0.822	0.853	[14,24,52]
κ_e	0.2–0.9	0.654	0.845	[14,24]
κ_a	0.2–0.8	0.505	0.509	[14,24]
κ_r	0.2–0.8	0.493	0.309	[14,24]
η_e	0.2–0.7	0.653	0.518	[14,24]
η_a	0.2–0.7	0.471	0.672	[14,24]
γ_a	0.05–0.4	0.2907	0.2907	[14,24]
γ_s	0.2–0.5	0.421	0.2268	[53]
γ_r	0.03–0.09	0.0652	0.0719	[54,55]
ν_h	0.1–0.5	0.35	0.209	[53]
ν_v	0.08–0.125	0.0911	0.115	[51,56]
B_v	500–100,000	18,000	51,047	Fitted
$1/\mu$	7–35	10.169	10.169	[51]
p	0.9–1	0.95	0.95	Fitted
a	1–10	1.8674	4.0325	Fitted
b	1–365	269.4	348.3	Fitted
τ	1–270	160	200	[31,32]

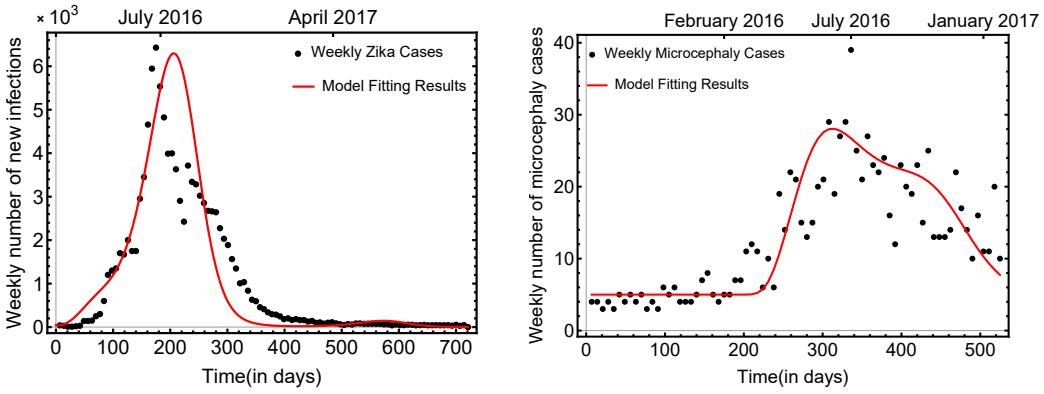

(**a**) (**b**)

Figure 4. The model (1) fits Colombian data between 2015 and 2017, with parameter values shown in Table 2. (**a**) Number of symptomatically infected. (**b**) Number of microcephaly cases.

3.2.2. The Impact of Sexual Transmission

Our model (1) allows us to estimate the effect of sexual transmission on infectious cases. Figure 5 depicts the number of symptomatically infected individuals in Colombia and the number of symptomatically infected estimated by our model ignoring sexual transmission. The results suggest that sexual transmission, a phenomenon previously unknown in mosquito-borne diseases, increased the total number of cases by several hundred.

Utilizing our model (1), we compare the symptomatic cases in adult females and the microcephaly cases with the corresponding numbers without sexual transmission (see Figure 6). Moreover, we observe a noticeable increase in the number of symptomatic cases in adult females and microcephaly cases with sexual transmission compared to those without it. This indicates that sexual transmission is playing a crucial role in spreading the

disease to this specific group of individuals. The results of our simulations suggest that sexual transmission is a significant contributor to the spread of the disease, and it should be taken into account in the development of effective control and prevention strategies. Using our model, we estimate that 9–18% of the total number of microcephaly cases in Colombia could be linked to Zika infection caused by sexual transmission.

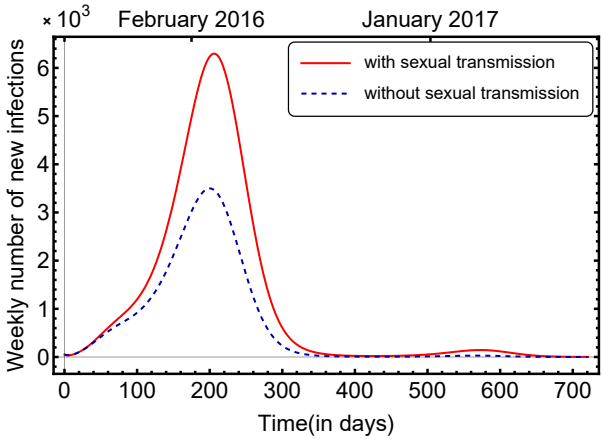

Figure 5. Number of the symptomatically infected and estimated number of symptomatically infected humans in the absence of sexual transmission.

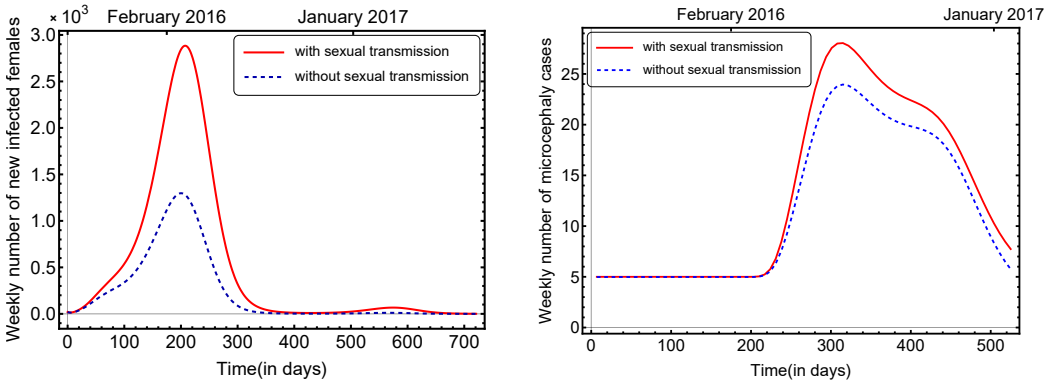

(**a**) Adult females (**b**) Microcephaly cases

Figure 6. Number of symptomatically infected adult females and estimated number of symptomatically infected adult females without sexual transmission in (**a**), and in (**b**) the number of microcephaly cases and estimated number of microcephaly cases without sexual transmission.

3.2.3. Sensitivity Analysis and Reproduction Numbers

To evaluate the dependency of the microcephaly number of cases on the controllable parameters of the model, we perform sensitivity analysis utilizing PRCC analysis. In Figure 7, we demonstrate the comparison of the PRCC values obtained for the parameters α_h, α_v, β, B_v and μ. The result of the sensitivity analysis suggests that the most crucial factors in the transmission of the disease, and consequently in the elevation of the number of microcephaly cases, are birth and death rates of mosquitoes. In comparison with these, the transmission rates, including sexual transmission, seem to have a somewhat smaller effect; however, they are still important factors in the transmission of Zika fever, as can also be seen from the simulations of the previous subsection. Based on the sensitivity analysis, we can assess that the most efficient ways to prevent Zika-related microcephaly cases are mosquito control and defence against mosquito bites.

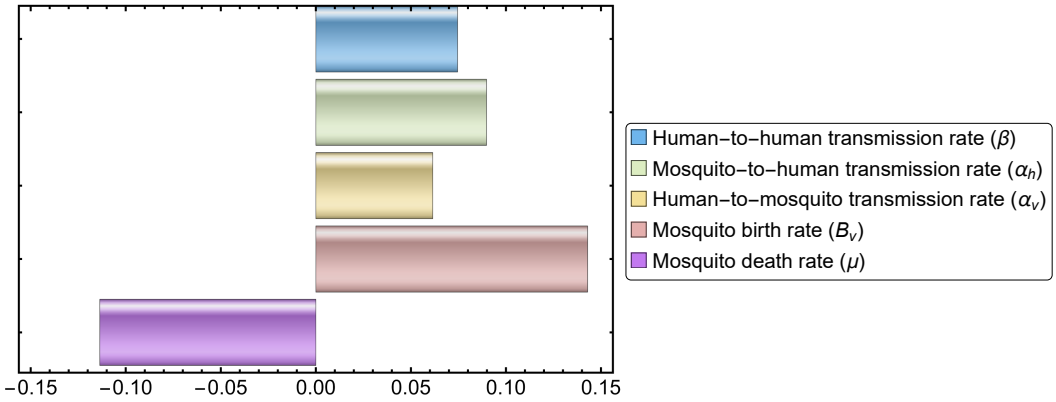

Figure 7. Partial rank correlation coefficients of the five parameters which can be subject to control measures. Parameters with positive (or negative) PRCC are positively (or negatively) correlated with the total number of cases.

Using the method established in [36], we obtained numerically $\mathcal{R}_0 \approx 0.974$ in the case of Colombia, as per the fact that the disease disappeared. We deduce a Formula (12) for the basic reproduction number, which provides the time-average reproduction number of the associated time-varying model (1) in any time point by substituting the values of the parameters into it, where the value of the time-dependent parameters is always taken at that given time point t. Moreover, Formula (11) provides us with the basic reproduction number of the associated time-constant model. To evaluate the dependence of the time-average basic reproduction number on the three controllable model parameters ($[\tilde{B}_v]$, $[\tilde{\alpha}_h]$, $[\tilde{\alpha}_v]$), the contour plots of the time-average reproduction number, $[\mathcal{R}_0]$, in terms of mosquito birth rate and mosquito-to-human transmission rate (left panel) and human-to-mosquito transmission rate (right panel), are shown in Figure 8, respectively. Similarly, the contour plots of the basic reproduction number, $\mathcal{R}_0^A$, of the autonomous model are given in Figure 9. The rest of the parameters are set as obtained in the fitting of symptomatically infected cases in Table 2. Figures 8 and 9 illustrate that the most significant measures to control the transmission of Zika involve decreasing mosquito birth rate, decreasing mosquito bites, personal bite surveillance and sexual contact protection.

Figure 10 shows the instantaneous reproduction number along with the number of symptomatically infected in Colombia, 2015–2017, showing that the number of infected individuals begins to decline when the instantaneous reproduction number goes below 1. The highest value of the instantaneous reproduction number is calculated to be about $\mathcal{R}_{inst} \approx 1.25$; this value can be contrasted with previous estimates. The authors in [16] estimated $\mathcal{R}_{inst} \approx 1.4$ for Brazil. Furthermore, the authors in [24] estimated $\mathcal{R}_{inst} \approx 1.47$ in Costa Rica, while in Suriname $\mathcal{R}_{inst} \approx 1.45$. These values are close to our results.

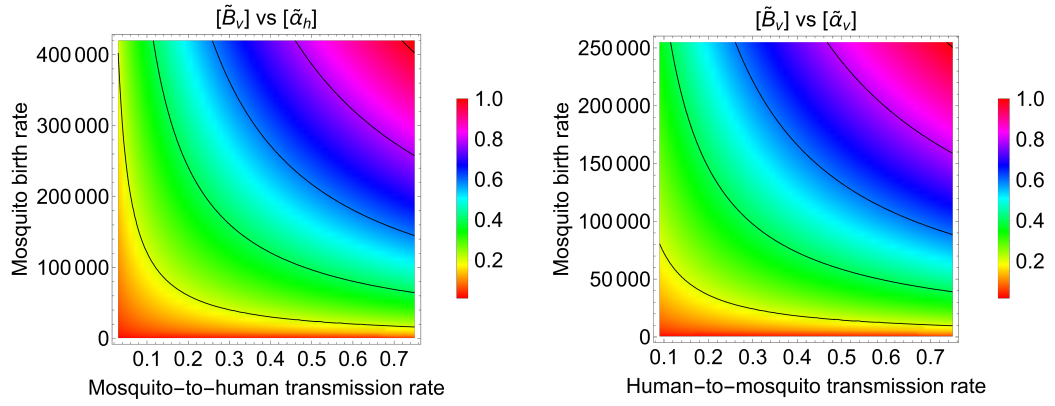

Figure 8. The contour plot of $[\mathcal{R}_0]$ as a function of $[\tilde{B}_v]$ and one of the three controllable parameters: mosquito-to-human transmission rate ($[\tilde{\alpha}_h]$) and human-to-mosquito transmission rate ($[\tilde{\alpha}_v]$).

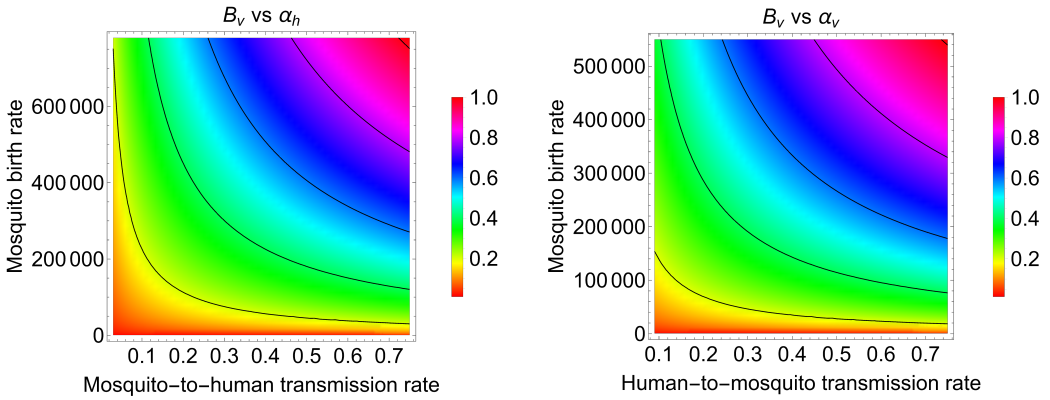

Figure 9. The contour plot of $\mathcal{R}_0^A$ as a function of B_v and one of the three controllable parameters: mosquito-to-human transmission rate (α_h) and human-to-mosquito transmission rate (α_v).

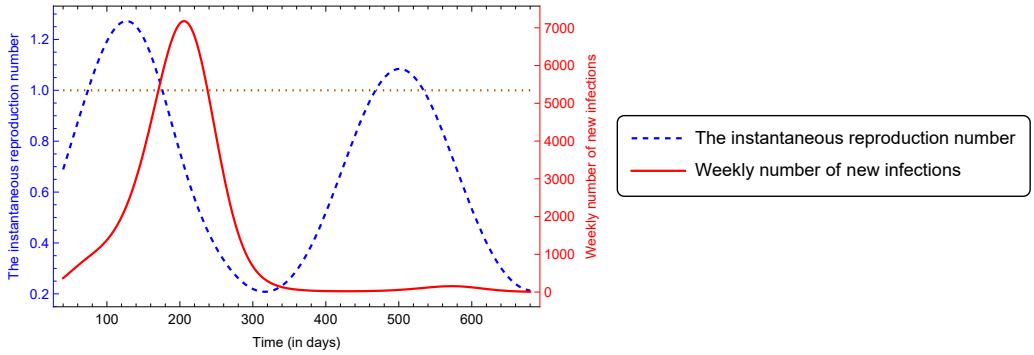

Figure 10. The instantaneous reproduction number and the number of symptomatically infected in Colombia, 2015–2017.

4. Discussion

We have developed a mathematical model for Zika virus disease transmission, with the particular aim of providing a better understanding of the effect on the most important health risk created by this disease, i.e., microcephaly. In our model, we tried to include most of the relevant characteristics of the Zika virus disease, namely, by improving our model given in [24], we consider both transmission ways (vectorial and sexual transmission), the role of asymptomatic carriers and time-dependent mosquito-related parameters due to the seasonality of weather. Our model also has its limitations: we have assumed an equal percentage of pregnant women in all female compartments, which might be different from reality. Furthermore, we have made the technical simplification of taking the time delay, τ, as a constant. Although periodic functions are a rather efficient tool to model the roughly periodic change of weather, they are, of course, unable to exactly describe the variance of weather. It is essential to acknowledge that the existence of a large number of parameters and broad intervals for their possible values makes it unlikely to identify a single set of parameters that precisely fits the data of the epidemic. The objective instead is to provide a credible estimate of the actual scenario and establish ranges for each parameter such that the true values have a high probability of falling within these intervals. This way, we can have a better understanding of the dynamics of the epidemic and make informed decisions accordingly.

We have established that the global dynamics of the system are described by the reproduction number: if $\mathcal{R}_0 < 1$, namely, we have shown global asymptotic stability of the disease-free periodic solution E_0, in this case, the disease goes extinct. If $\mathcal{R}_0 > 1$, the disease becomes endemic in the population. We also provided numerical simulations in accordance with these theoretical results (see Figure 3).

As an example of the application of the model, we fitted it to the number of Zika cases and the number of microcephaly cases in Colombia. Using the results of the fitting and partial rank correlation coefficients analysis, we tried to assess which phenomena are the main drivers of the increase in microcephaly cases. We have estimated the contribution of sexual transmission to the increase in the number of cases to find that about 9–18% of the microcephaly cases might be attributed to this sexual transmission, a novel phenomenon for mosquito-borne diseases. Our results indicate that the sexual transmission rate increases the number of infected adult females and consequently increases the risk of microcephaly due to vertical transmission.

The basic reproduction number of the time-periodic model, the instantaneous reproduction number and the time-dependent reproduction number were calculated. The results are consistent with the extinction of the ZIKV epidemic in Colombia. By calculating both the time-average reproduction number for the time-period model and the reproduction number of the time-constant model, we determine the dependency of the basic reproduction number on the model's controllable parameters. We obtain that mosquito birth and biting rates are the most significant factors in the transmission of Zika and the increase of microcephaly cases after the end of the outbreak in Colombia; however, the sexual transmission rate also has an important impact on the spread of the disease.

Based on our results, we may conclude that mosquito control, protection against mosquito bites and sexual contact protection during the pregnancy period are the most successful ways to prevent Zika-related microcephaly cases.

Author Contributions: Conceptualization, M.A.I. and A.D.; methodology, M.A.I. and A.D.; software, M.A.I. and A.D.; validation, M.A.I. and A.D.; formal analysis, M.A.I.; investigation, M.A.I. and A.D.; writing—original draft preparation, M.A.I. and A.D.; writing—review and editing, M.A.I. and A.D.; visualization, M.A.I. and A.D. All authors have read and agreed to the published version of the manuscript.

Funding: This research was supported by project TKP2021-NVA-09, implemented with the support provided by the Ministry of Innovation and Technology of Hungary from the National Research, Development and Innovation Fund, financed under the TKP2021-NVA funding scheme. M. A. Ibrahim was supported by project no. 129877 of the National Research, Development and Innovation Office of Hungary, financed under the KKP_19 funding scheme and by a fellowship from the Egyptian government in the long-term mission system. A. Dénes acknowledges the support of the National Laboratory for Health Security, RRF-2.3.1-21-2022-00006 and of projects no. 128363 and no. 125119 of the National Research, Development and Innovation Office of Hungary, financed under the PD_18 and SNN_17 funding schemes, respectively.

Institutional Review Board Statement: Not applicable.

Informed Consent Statement: Not applicable.

Data Availability Statement: Not applicable.

Conflicts of Interest: The authors declare no conflict of interest.

References

1. Petersen, L.R.; Jamieson, D.J.; Powers, A.M.; Honein, M.A. Zika virus. *N. Engl. J. Med.* **2016**, *374*, 1552–1563. [CrossRef] [PubMed]
2. Magalhaes, T.; Foy, B.D.; Marques, E.T.; Ebel, G.D.; Weger-Lucarelli, J. Mosquito-borne and sexual transmission of Zika virus: Recent developments and future directions. *Virus Res.* **2018**, *254*, 1–9. [CrossRef] [PubMed]
3. Mead, P.S.; Duggal, N.K.; Hook, S.A.; Delorey, M.; Fischer, M.; Olzenak McGuire, D.; Becksted, H.; Max, R.J.; Anishchenko, M.; Schwartz, A.M.; et al. Zika virus shedding in semen of symptomatic infected men. *N. Engl. J. Med.* **2018**, *378*, 1377–1385. [CrossRef] [PubMed]
4. Dick, G.W.; Kitchen, S.F.; Haddow, A.J. Zika virus (I). Isolations and serological specificity. *Trans. R. Soc. Trop. Med. Hyg.* **1952**, *46*, 509–520. [CrossRef] [PubMed]

5. World Health Organization. Zika Virus, Microcephaly and Guillain–Barré Syndrome. Situation Report. Available online: http://apps.who.int/iris/bitstream/handle/10665/204961/zikasitrep_7Apr2016_eng.pdf (accessed on 15 February 2023).
6. European Centre for Disease Prevention and Control. Zika Virus Epidemic in the Americas: Potential Association with Microcephaly and Guillain–Barré (2015) Rapid Risk Assessment. Available online: ecdc.europa.eu/en/publications/Publications/zika-virus-americas-association-with-microcephaly-rapid-risk-assessment.pdf (accessed on 15 February 2023).
7. Romero, S. Alarm Spreads in Brazil over a Virus and a Surge in Malformed Infants. Available online: https://www.nytimes.com/2015/12/31/world/americas/alarm-spreads-in-brazil-over-a-virus-and-a-surge-in-malformed-infants.html?smid=nytcore-ipad-share&smprod=nytcore-ipad&_r=1 (accessed on 15 February 2023).
8. Colombia National Institute of Health. Epidemiological Bulletin. EW 52 of 2016. Available online: http://www.ins.gov.co/boletin-epidemiologico/Boletn%20Epidemiolgico/2016%20Bolet%C3%ADn%20epidemiol%C3%B3gico%20semana%2052%20-.pdf (accessed on 15 February 2023).
9. Colombia National Institute of Health. Epidemiological Bulletin. EW 33 of 2017. Available online: http://www.ins.gov.co/boletinepidemiologico/Boletn%20Epidemiolgico/2017%20Bolet%C3%ADn%20epidemiol%C3%B3gico%20semana%2033.pdf (accessed on 15 February 2023).
10. de Araújo, T.V.B.; Ximenes, R.A.A.; de Barros Miranda-Filho, D.; Souza, W.V.; Montarroyos, U.R.; de Melo, A.P.L.; Valongueiro, S.; de Albuquerque, M.F.P.M.; Braga, C.; Filho, S.P.B.; et al. Association between microcephaly, Zika virus infection, and other risk factors in Brazil: Final report of a case-control study. *Lancet Infect. Dis.* **2018**, *18*, 328–336. [PubMed]
11. Brady, O.J.; Osgood-Zimmerman, A.; Kassebaum, N.J.; Ray, S.E.; de Araújo, V.E.; da Nóbrega, A.A.; Frutuoso, L.C.; Lecca, R.C.; Stevens, A.; Zoca de Oliveira, B.; et al. The association between Zika virus infection and microcephaly in Brazil 2015–2017: An observational analysis of over 4 million births. *PLoS Med.* **2019**, *16*, e1002755. [CrossRef] [PubMed]
12. Méndez, N.; Oviedo-Pastrana, M.; Mattar, S.; Caicedo-Castro, I.; Arrieta, G. Zika virus disease, microcephaly and Guillain-Barré syndrome in Colombia: Epidemiological situation during 21 months of the Zika virus outbreak, 2015–2017. *Arch. Public Health* **2017**, *75*, 65 . [CrossRef]
13. Song, B.H.; Yun, S.I.; Woolley, M.; Lee, Y.M. Zika virus: History, epidemiology, transmission, and clinical presentation. *J. Neuroimmunol.* **2017**, *308*, 50–64. [CrossRef]
14. Gao, D.; Lou, Y.; He, D.; Porco, T.C.; Kuang, Y.; Chowell, G.; Ruan, S. Prevention and control of Zika as a mosquito-borne and sexually transmitted disease: A mathematical modeling analysis. *Sci. Rep.* **2016**, *6*, 28070. [CrossRef]
15. Sasmal, S.K.; Ghosh, I.; Huppert, A.; Chattopadhyay, J. Modeling the spread of Zika virus in a stage-structured population: Effect of sexual transmission. *Bull. Math. Biol.* **2018**, *80*, 3038–3067. [CrossRef]
16. Saad-Roy, C.; Ma, J.; Van den Driessche, P. The effect of sexual transmission on Zika virus dynamics. *J. Math. Biol.* **2018**, *77*, 1917–1941. [CrossRef]
17. Caminade, C.; Turner, J.; Metelmann, S.; Hesson, J.C.; Blagrove, M.S.; Solomon, T.; Morse, A.P.; Baylis, M. Global risk model for vector-borne transmission of Zika virus reveals the role of El Niño 2015. *Proc. Natl. Acad. Sci. USA* **2017**, *114*, 119–124. [CrossRef] [PubMed]
18. Mordecai, E.A.; Cohen, J.M.; Evans, M.V.; Gudapati, P.; Johnson, L.R.; Lippi, C.A.; Miazgowicz, K.; Murdock, C.C.; Rohr, J.R.; Ryan, S.J.; et al. Detecting the impact of temperature on transmission of Zika, dengue, and chikungunya using mechanistic models. *PLoS Neglected Trop. Dis.* **2017**, *11*, e0005568. [CrossRef] [PubMed]
19. Wang, W.; Zhou, M.; Zhang, T.; Feng, Z. Dynamics of a Zika virus transmission model with seasonality and periodic delays. *Commun. Nonlinear Sci. Numer. Simul.* **2023**, *116*, 106830. [CrossRef]
20. Zhu, G.; Shi, Y.; Li, Y.; Xiao, G.; Xiao, J.; Liu, Q. Model-Based Projection of Zika Infection Risk with Temperature Effect: A Case Study in Southeast Asia. *Bull. Math. Biol.* **2022**, *84*, 92. [CrossRef]
21. Suparit, P.; Wiratsudakul, A.; Modchang, C. A mathematical model for Zika virus transmission dynamics with a time-dependent mosquito biting rate. *Theor. Biol. Med Model.* **2018**, *15*, 11. [CrossRef]
22. Ibrahim, M.A.; Dénes, A. Threshold dynamics in a model for Zika virus disease with seasonality. *Bull. Math. Biol.* **2021**, *83*, 27. [CrossRef]
23. Agusto, F.B.; Bewick, S.; Fagan, W. Mathematical model of Zika virus with vertical transmission. *Infect. Dis. Model.* **2017**, *2*, 244–267. [CrossRef]
24. Dénes, A.; Ibrahim, M.A.; Oluoch, L.; Tekeli, M.; Tekeli, T. Impact of weather seasonality and sexual transmission on the spread of Zika fever. *Sci. Rep.* **2019**, *9*, 17055. [CrossRef]
25. Foy, B.D.; Kobylinski, K.C.; Foy, J.L.C.; Blitvich, B.J.; da Rosa, A.T.; Haddow, A.D.; Lanciotti, R.S.; Tesh, R.B. Probable non–vector-borne transmission of Zika virus, Colorado, USA. *Emerg. Infect. Dis.* **2011**, *17*, 880. [CrossRef]
26. Centers for Disease Control and Prevention, National Center on Birth Defects and Developmental Disabilities. Facts about Microcephaly. Available online: www.cdc.gov/ncbddd/birthdefects/microcephaly.html (accessed on 15 February 2023).
27. Bakary, T.; Boureima, S.; Sado, T. A mathematical model of malaria transmission in a periodic environment. *J. Biol. Dyn.* **2018**, *12*, 400–432. [CrossRef]

28. Instituto Nacional de Salud (Colombia). Boletín Epidemiológico. Bogotá, D. C.: 2017. Available online: http://www.ins.gov.co/boletin-epidemiologico/Paginas/default.aspx (accessed on 15 February 2023).
29. Ministerio de Salud y Protección Social—Instituto Nacional de Salud (Colombia) Circular Conjunta Externa N° 00000061 de 2015. Vigilancia de la Fiebre por Virus Zika (ZIKV) en su fase II Epidémica y Fortalecimiento de la Prevención de la Fiebre por Virus Zika en Grupos de Riesgo. Bogotá, D.C. 2017. Available online: http://www.ins.gov.co/Noticias/ZIKA/Circular%20Conj%20061%202015%20Fiebre%20zika.pdf (accessed on 15 February 2023).
30. Ministerio de Salud y Protección Social—Instituto Nacional de Salud (Colombia). Protocolo de Vigilancia en Salud Pública: Enfermedad por Virus Zika. Bogotá, D.C. 2017. Available online: http://bvs.minsa.gob.pe/local/MINSA/3449.pdf (accessed on 15 February 2023).
31. Pan American Health Organization. Countries and Territories with Autochthonous Transmission of Zika Virus in the Americas Reported in 2015–2017. Available online: https://www.paho.org/hq/index.php?option=com_Content&view=article&id=11603:countries-and-territories-with-autochthonous-transmission-of-zika-virus-in-the-americas-reported-in-2015-2017&Itemid=41696&lang=en (accessed on 15 February 2023).
32. Pan American Health Organization. Zika–Epidemiological Report Colombia. Available online: https://www.paho.org/hq/dmdocuments/2017/2017-phe-zika-situation-report-col.pdf (accessed on 15 February 2023).
33. McKay, M.D.; Beckman, R.J.; Conover, W.J. A comparison of three methods for selecting values of input variables in the analysis of output from a computer code. *Technometrics* **2000**, *42*, 55–61. [CrossRef]
34. Blower, S.M.; Dowlatabadi, H. Sensitivity and uncertainty analysis of complex models of disease transmission: An HIV model, as an example. *Int. Stat. Rev. Int. Stat.* **1994**, *62*, 229–243. [CrossRef]
35. Wang, W.; Zhao, X.Q. Threshold dynamics for compartmental epidemic models in periodic environments. *J. Dyn. Differ. Equations* **2008**, *20*, 699–717. [CrossRef]
36. Mitchell, C.; Kribs, C. A comparison of methods for calculating the basic reproductive number for periodic epidemic systems. *Bull. Math. Biol.* **2017**, *79*, 1846–1869. [CrossRef] [PubMed]
37. Hale, J.K.; Lunel, S.M.V. *Introduction to Functional Differential Equations*; Springer Science & Business Media: New York, NY, USA, 2013; Volume 99.
38. Smith, H.L. *Monotone Dynamical Systems: An Introduction to the Theory of Competitive and Cooperative Systems: An Introduction to the Theory of Competitive and Cooperative Systems*; American Mathematical Society: Providence, RI, USA, 2008.
39. Zhao, X.Q. Basic reproduction ratios for periodic compartmental models with time delay. *J. Dyn. Differ. Equations* **2017**, *29*, 67–82. [CrossRef]
40. Diekmann, O.; Heesterbeek, J.; Roberts, M.G. The construction of next-generation matrices for compartmental epidemic models. *J. R. Soc. Interface* **2010**, *7*, 873–885. [CrossRef]
41. Zhao, X.Q. *Dynamical Systems in Population Biology*; Springer: Cham, Switzerland, 2003; Volume 16.
42. Lou, Y.; Zhao, X.Q. A theoretical approach to understanding population dynamics with seasonal developmental durations. *J. Nonlinear Sci.* **2017**, *27*, 573–603. [CrossRef]
43. Walter, W. On strongly monotone flows. *Ann. Pol. Math.* **1997**, *66*, 269–274. [CrossRef]
44. Liang, X.; Zhao, X.Q. Asymptotic speeds of spread and traveling waves for monotone semiflows with applications. *Commun. Pure Appl. Math. J. Issued Courant Inst. Math. Sci.* **2007**, *60*, 1–40. [CrossRef]
45. Wang, X.; Zhao, X.Q. Dynamics of a time-delayed Lyme disease model with seasonality. *SIAM J. Appl. Dyn. Syst.* **2017**, *16*, 853–881. [CrossRef]
46. Wang, X.; Zhao, X.Q. A periodic vector-bias malaria model with incubation period. *SIAM J. Appl. Math.* **2017**, *77*, 181–201. [CrossRef]
47. Zhang, Y.; Zhao, X.Q. A reaction-diffusion Lyme disease model with seasonality. *SIAM J. Appl. Math.* **2013**, *73*, 2077–2099. [CrossRef]
48. Xu, D.; Zhao, X.Q. Dynamics in a periodic competitive model with stage structure. *J. Math. Anal. Appl.* **2005**, *311*, 417–438. [CrossRef]
49. World Health Organization. WHO Global Health Observatory Data Repository. Crude Birth and Death Rate. Data by Country. Available online: http://apps.who.int/gho/data/node.main.CBDR107?lang=en (accessed on 15 February 2023).
50. Chikaki, E.; Ishikawa, H. A dengue transmission model in Thailand considering sequential infections with all four serotypes. *J. Infect. Dev. Ctries.* **2009**, *3*, 711–722. [CrossRef] [PubMed]
51. Andraud, M.; Hens, N.; Marais, C.; Beutels, P. Dynamic epidemiological models for dengue transmission: A systematic review of structural approaches. *PLoS ONE* **2012**, *7*, e49085. [CrossRef] [PubMed]
52. Duffy, M.R.; Chen, T.H.; Hancock, W.T.; Powers, A.M.; Kool, J.L.; Lanciotti, R.S.; Pretrick, M.; Marfel, M.; Holzbauer, S.; Dubray, C.; et al. Zika virus outbreak on Yap Island, federated states of Micronesia. *N. Engl. J. Med.* **2009**, *360*, 2536–2543. [CrossRef] [PubMed]
53. Bearcroft, W. Zika virus infection experimentally induced in a human volunteer. *Trans. R. Soc. Trop. Med. Hyg.* **1956**, *50*, 442–448. [CrossRef]
54. Gourinat, A.C.; O'Connor, O.; Calvez, E.; Goarant, C.; Dupont-Rouzeyrol, M. Detection of Zika virus in urine. *Emerg. Infect. Dis.* **2015**, *21*, 84. [CrossRef]

55. Musso, D.; Roche, C.; Robin, E.; Nhan, T.; Teissier, A.; Cao-Lormeau, V.M. Potential sexual transmission of Zika virus. *Emerg. Infect. Dis.* **2015**, *21*, 359. [CrossRef]
56. Boorman, J.; Porterfield, J. A simple Technique for Infection of Mosquitoes with Viruses. Transmission of Zika Yirus. *Trans. R. Soc. Trop. Med. Hyg.* **1956**, *50*, 238–242. [CrossRef] [PubMed]